APPLICATIONS OF POWER SERIES SOLUTIONS OF MEMBRANE EQUILIBRIUM EQUATIONS TO THE OPTICAL EVALUATION OF MEMBRANE MIRRORS WITH CURVATURE

James M. Wilkes

December 1998

Final Report

APPROVED FOR PUBLIC RELEASE; DISTRIBUTION IS UNLIMITED.

AIR FORCE RESEARCH LABORATORY
Directed Energy Directorate
3550 Aberdeen Ave SE
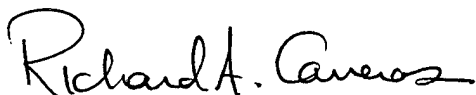**AIR FORCE MATERIEL COMMAND**
KIRTLAND AIR FORCE BASE, NM 87117-5776

19990203 084

AFRL-DE-PS-TR-1998-1069

RICHARD A. CARRERAS
Project Manager

FOR THE COMMANDER

STANLEY R. CZYZAK, DR3
Chief, DEBS

R. EARL GOOD, SES
Director, Directed Energy Directorate

REPORT DOCUMENTATION PAGE	Form Approved OMB No. 074-0188

Public reporting burden for this collection of information is estimated to average 1 hour per response, including the time for reviewing instructions, searching existing data sources, gathering and maintaining the data needed, and completing and reviewing this collection of information. Send comments regarding this burden estimate or any other aspect of this collection of information, including suggestions for reducing this burden to Washington Headquarters Services, Directorate for Information Operations and Reports, 1215 Jefferson Davis Highway, Suite 1204, Arlington, VA 22202-4302, and to the Office of Management and Budget, Paperwork Reduction Project (0704-0188), Washington, DC 20503

1. AGENCY USE ONLY (Leave blank)	2. REPORT DATE Dec 98	3. REPORT TYPE AND DATES COVERED Technical Report Dec 97-Dec 98	

4. TITLE AND SUBTITLE
Applications of Power Series Solutions of Membrane Equilibrium Equations to the Optical Evaluation of Membrane Mirrors with Curvature

5. FUNDING NUMBERS
PE: 62601F
PR: 3326
TA: LH
WU: 02

6. AUTHOR(S)
James M. Wilkes

7. PERFORMING ORGANIZATION NAME(S) AND ADDRESS(ES)
Air Force Research Laboratory/DEBS
3550 Aberdeen Ave SE
Kirtland AFB, NM 87117-5776

8. PERFORMING ORGANIZATION REPORT NUMBER
AFRL-DE-PS-TR-1998-1069

9. SPONSORING / MONITORING AGENCY NAME(S) AND ADDRESS(ES)

10. SPONSORING / MONITORING AGENCY REPORT NUMBER

11. SUPPLEMENTARY NOTES

12a. DISTRIBUTION / AVAILABILITY STATEMENT
Approved for public release; distribution is unlimited.

12b. DISTRIBUTION CODE

13. ABSTRACT *(Maximum 200 Words)*
Power series solutions of the Hencky-Campbell equilibrium equations for an initially planar circular membrane in a state of uniform pre-strain are used to analyze the performance of an in-house laboratory membrane mirror curved by a uniform vacuum pressure applied to one side. The results provide theoretical verification of the improvement in surface figure achievable by controlling the amount of pre-strain. In particular, a pre-strain of only 0.25%, corresponding to a uniform radial displacement of the edge of an 11-inch diameter membrane mirror by about 0.014 inches, is predicted to achieve nearly 95% reduction in the maximum deviation of an f/8 membrane from a reference sphere. These results are in good agreement with laboratory measurements of spherical aberration using a Hartmann wavefront sensor. The model was also used in an extensive investigation of the effects of control parameters (pressure and pre-strain) on the improvement of surface figure for lower f-number systems. The results indicate that comparable improvement in systems of f-number less than f/6 would require membrane materials capable of withstanding pre-strains on the order of 2.0% or greater.

14. SUBJECT TERMS
membrane theory, membrane mirrors, optical systems design

15. NUMBER OF PAGES
36

16. PRICE CODE

17. SECURITY CLASSIFICATION OF REPORT Unclassified	18. SECURITY CLASSIFICATION OF THIS PAGE Unclassified	19. SECURITY CLASSIFICATION OF ABSTRACT Unclassified	20. LIMITATION OF ABSTRACT Unlimited

NSN 7540-01-280-5500

i

Standard Form 298 (Rev. 2-89)
Prescribed by ANSI Std. Z39-18
298-102

Contents

List of Figures

I. INTRODUCTION

An initially flat circular membrane forming one end of a cylindrical vacuum chamber, and clamped along the rim, deforms under vacuum to a surface whose shape has been found to be less than ideal for optical applications. Deviations from an ideal paraboloid or sphere are greater than 100λ at optical wavelengths λ, even for membrane (paraxial) f-numbers as high as $f/8$. The work reported here was carried out in support of an in-house laboratory effort to demonstrate the improvement of this shape by introducing a controllable strain, independent of the vacuum pressure used to produce the membrane curvature. These experiments were performed on a Upilex membrane mounted on two concentric cylinders to form one end of two independently controlled vacuum chambers. When a vacuum is created in the interior of the outer annulus ($p_o < p_{atm}$, where p_{atm} is laboratory atmospheric pressure), with no vacuum on the inner cylinder ($p = p_{atm}$), the membrane is free to move outward across the inner ring, creating a strain in the inner membrane. For a given vacuum pressure $p < p_{atm}$ on the inner cylinder, this "pre-strain" favorably affects the final shape of the inner membrane surface compared to the shape it would attain with no pre-strain (note that when $p < p_{atm}$, the annulus pressure may change to some new value p'_0 due to migration of membrane material back across the inner ring). The amount of pre-strain can be controlled by the annulus pressure, affording a degree of control over the final shape of the inner membrane. Details of this "rim-controlled" membrane and its use in a simple optical system were presented in references [6], [7], and [9]. The design of the membrane mounting is illustrated in Figure 1.
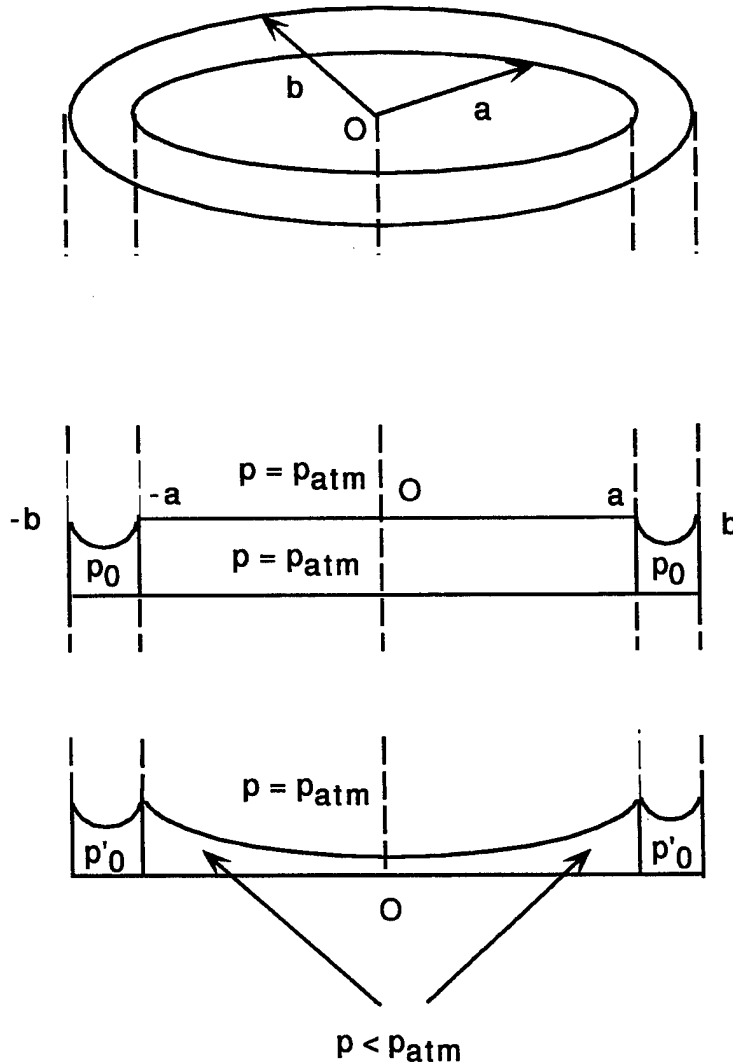

FIG. 1. In-House Laboratory Membrane Mirror

The goals of the modelling effort described in this report were to provide theoretical verification of pre-strain control of a membrane surface, and to investigate effects of the control parameters (inner membrane pressure p and pre-strain ϵ) on the final shape. The boundary value problem corresponding to the rim-controlled membrane mirror used in our laboratory experiments is, however, rather formidable, and to the author's knowledge its solution has not been given in the literature. We have thus opted to instead examine a different boundary value problem whose solution is fairly well-known, and which corresponds to an experimental situation similar in some respects to the one in our laboratory. Results obtained from this solution will be shown to be in qualitative agreement with measurements made on the laboratory membrane, and can thus serve as a guide in optical designs using the membrane as a mirror. In addition, the next generation of experiments at this laboratory are expected to involve a membrane mounting that more nearly resembles the one described by the boundary value problem solved here.

As a quick review of the history of this problem, we note that in 1915 Hencky [5] proposed a system of equations for determining the equilibrium configuration of an initially plane circular membrane deformed by an axially symmetric constant pressure load. They are essentially von Kármán's nonlinear plate equations [11] specialized to zero flexural rigidity D (for a clear and careful discussion of the von Kármán equations, see [3]). Hencky derived power series solutions for the stress, strain, and displacement vector components for the case of an initially unstressed membrane. In 1956 Campbell [1] generalized Hencky's problem to include an initial tension in the membrane. In Sections II-V we give a detailed description of the setting for the Hencky-Campbell problem, and show that it is equivalent to the problem of a membrane subjected to an initial purely radial displacement of its edge, then clamped at the original radius before being deformed by a uniform pressure. This boundary value problem is illustrated in Figure 2, where the differences between the laboratory membrane mounting and the one modeled by the Hencky-Campbell theory are apparent, i.e., the Hencky-Campbell membrane is clamped at the inner ring after pre-straining it by a radial displacement of its edge, and is then pressurized, while the laboratory membrane can slip back over the inner ring when it is pressurized, after pre-straining it by the annulus pressure.
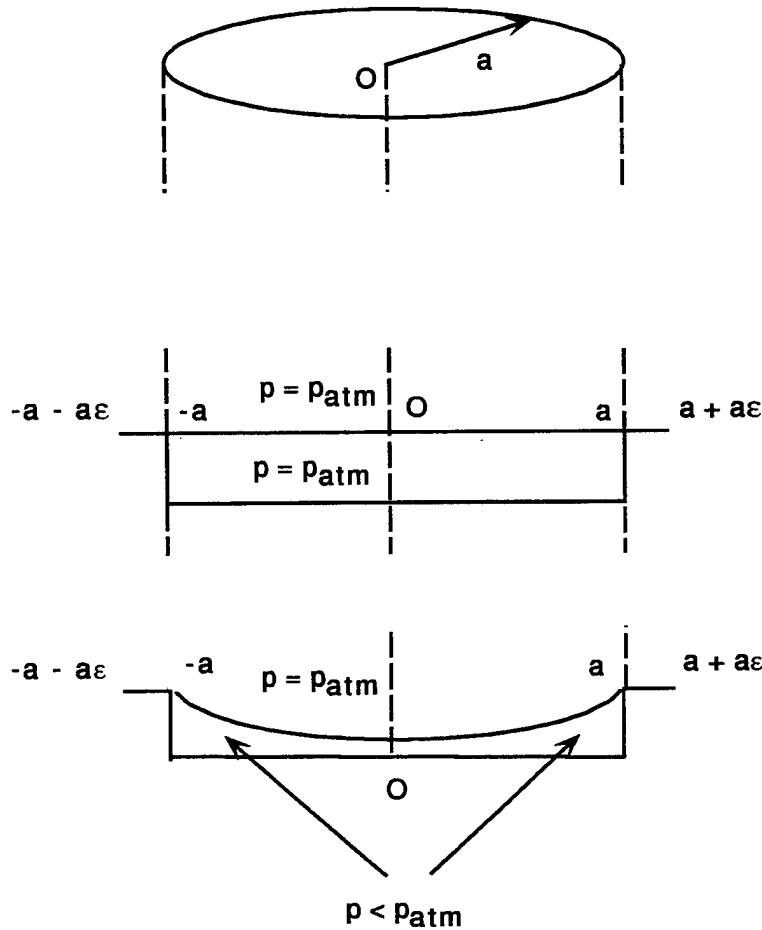

FIG. 2. Hencky-Campbell Membrane Model

Sections VI and VII are concerned with the elasto-mechanical properties of the membrane derived from the Hencky-Campbell theory, while Section VIII begins a discussion of relations between these properties and some of the optical parameters of the problem.

II. REFERENCE CONFIGURATION

We consider a body, henceforth referred to as a membrane, whose reference configuration is a thin circular disk of radius a and thickness $h << a$. An arbitrary point P of the reference configuration can be specified by either its Cartesian coordinates $\{X, Y, Z\}$, or its cylindrical coordinates (R, Θ, Z). The *middle plane* of the membrane is the plane $Z = 0$, and we take the origin of coordinates to be the center O of the circle of radius a in this plane. We assume given a fixed orthonormal Cartesian basis $\{i, j, k\}$ at O. The position vector of P with respect to O is given by

$$X = X i + Y j + Z k. \tag{2.1}$$

The cylindrical and Cartesian coordinates of P are related by the following transformation equations:

$$X = R \cos \Theta, \quad Y = R \sin \Theta, \quad Z = Z, \tag{2.2}$$

hence the position vector can be written in terms of cylindrical coordinates as

$$X = R \cos \Theta \, i + R \sin \Theta \, j + Z k. \tag{2.3}$$

We introduce orthonormal basis vectors $\{E_R, E_\Theta, E_Z\}$ associated with the cylindrical coordinates, and defined in terms of the fixed basis vectors by

$$E_R(\Theta) = \cos \Theta \, i + \sin \Theta \, j, \quad E_\Theta(\Theta) = -\sin \Theta \, i + \cos \Theta \, j, \quad E_Z = k, \tag{2.4}$$

in terms of which the position vector can be written as

$$X(R, \Theta, Z) = R \, E_R(\Theta) + Z \, E_Z. \tag{2.5}$$

III. ASSUMPTIONS ON THE DEFORMATION

Under a uniform pressure p, a point P of the reference configuration is deformed to a new point P'. The set of all such points defines the deformed configuration. The point P' of the deformed configuration has Cartesian coordinates $\{x, y, z\}$ and cylindrical coordinates (r, θ, z). The position vector of P' with respect to the origin O at the center of the membrane is thus given in the fixed Cartesian basis by

$$x = x i + y j + z k = = r \cos \theta \, i + r \sin \theta \, j + z k, \tag{3.1}$$

where the cylindrical and Cartesian coordinates are related by

$$x = r \cos \theta, \quad y = r \sin \theta, \quad z = z. \tag{3.2}$$

The orthonormal basis vectors $\{e_r, e_\theta, e_z\}$ associated with the cylindrical coordinates on the deformed configuration are defined by

$$e_r(\theta) = \cos \theta \, i + \sin \theta \, j, \quad e_\theta(\theta) = -\sin \theta \, i + \cos \theta \, j, \quad e_z = k \equiv E_Z, \tag{3.3}$$

in terms of which the position vector can be written as

$$x = r \, e_r + z \, e_z. \tag{3.4}$$

The *displacement vector* u relates the position vector X of P in the reference configuration to the position vector x of the point P' to which P is displaced by the deformation, i.e., $u \equiv x - X$, hence

$$x = X + u. \tag{3.5}$$

3

We write the displacement vector in the cylindrical basis $\{E_R, E_\Theta, E_Z\}$ of the reference configuration as

$$u = U_R\,E_R + U_\Theta\,E_\Theta + U_Z\,E_Z, \tag{3.6}$$

where the orthonormal cylindrical basis vectors are related to the fixed Cartesian basis vectors by (2.4). Thus, (3.5) can be written as

$$
\begin{aligned}
x\,i + y\,j + z\,k &= X\,i + Y\,j + Z\,k + U_R\,E_R + U_\Theta\,E_\Theta + U_Z\,E_Z \\
&= X\,i + Y\,j + Z\,k + U_R\,(\cos\Theta\,i + \sin\Theta\,j) + U_\Theta\,(-\sin\Theta\,i + \cos\Theta\,j) + U_Z\,k, \\
&= (X + U_R\cos\Theta - U_\Theta\sin\Theta)\,i + (Y + U_R\sin\Theta + U_\Theta\cos\Theta)\,j + (Z + U_Z)\,k.
\end{aligned}
\tag{3.7}
$$

From (3.7) we obtain the following relations between the *Cartesian coordinates* of the two *position* vectors, and the *cylindrical components* of the *displacement* vector:

$$x = X + U_R\cos\Theta - U_\Theta\sin\Theta, \tag{3.8a}$$

$$y = Y + U_R\sin\Theta + U_\Theta\cos\Theta, \tag{3.8b}$$

$$z = Z + U_Z. \tag{3.8c}$$

Substituting from (2.2) and (3.2) into the first two equations of (3.8), we obtain

$$r\cos\theta = (R + U_R)\cos\Theta - U_\Theta\sin\Theta, \tag{3.9a}$$

$$r\sin\theta = (R + U_R)\sin\Theta + U_\Theta\cos\Theta. \tag{3.9b}$$

These equations can be solved for the deformed configuration cylindrical coordinates in terms of the reference configuration cylindrical coordinates and displacement vector components as follows: first, multiply the first equation by $\cos\Theta$ and the second by $\sin\Theta$, and add the results to get (using the trigonometric identity for the cosine of the difference of two angles) $r\cos(\Theta - \theta) = R + U_R$; second, multiply the first equation by $-\sin\Theta$ and the second by $\cos\Theta$, and add to get $r\sin(\Theta - \theta) = U_\Theta$. From these two results one easily obtains

$$r = \sqrt{(R + U_R)^2 + U_\Theta^2}\,, \tag{3.10a}$$

$$\theta = \Theta - \tan^{-1}\left(\frac{U_\Theta}{R + U_R}\right). \tag{3.10b}$$

We assume that the deformation of the membrane from its reference configuration to its deformed configuration is described mathematically by one-to-one invertible mappings between the coordinates of points in the two configurations, e.g., between their cyindrical coordinates:

$$r = f_r(R, \Theta, Z), \quad \theta = f_\theta(R, \Theta, Z), \quad z = f_z(R, \Theta, Z). \tag{3.11}$$

We immediately restrict consideration to deformations in which the cylindrical coordinate Θ of any point in the reference configuration remains the *same* after the deformation, i.e., we assume that the second equation of (3.11) is the identity mapping

$$\theta = \Theta. \tag{3.12}$$

Furthermore, we restrict consideration to deformations that are *independent* of this angular coordinate. Equations (3.11) thus reduce to a pair of mappings depending only on the other two coordinates:

$$r = f_r(R, Z), \quad z = f_z(R, Z). \tag{3.13}$$

Under these assumptions of axisymmetric deformation, equations (3.12) and (3.10b) imply that

$$U_\Theta = 0, \tag{3.14}$$

4

hence the relation (3.10a) between radial coordinates in the two configurations simplifies considerably to

$$r = f_r(R, Z) = R + U_R(R, Z).$$ (3.15)

The relation (3.8c) between the vertical coordinates is unchanged:

$$z = f_z(R, Z) = Z + U_Z(R, Z),$$ (3.16)

and the displacement vector reduces to

$$\boldsymbol{u}(R, \Theta, Z) = U_R(R, Z)\,\boldsymbol{E}_R(\Theta) + U_Z(R, Z)\,\boldsymbol{E}_Z.$$ (3.17)

Assumption (3.12) implies that the orthonormal basis vectors $\{e_R, e_\Theta, e_Z\}$ on the deformed configuration are the same as those on the reference configuration, i.e.,

$$\boldsymbol{e}_r(\theta) = \boldsymbol{e}_r(\Theta) = \boldsymbol{E}_R(\Theta), \quad \boldsymbol{e}_\theta(\theta) = \boldsymbol{e}_\theta(\Theta) = \boldsymbol{E}_\Theta(\Theta), \quad \boldsymbol{e}_z = \boldsymbol{E}_Z = \boldsymbol{k}.$$ (3.18)

IV. HENCKY'S EQUATIONS

Hencky's equations describe the equilibrium state of the *middle surface* of the deformed membrane, i.e., the *image* under the deformation of the middle plane $Z = 0$. Setting $Z = 0$ in (3.15) and (3.16), we write the equations describing the middle surface as

$$r = F(R) = R + U(R), \quad \text{where} \quad F(R) \equiv f_r(R, 0) \quad \text{and} \quad U(R) \equiv U_R(R, 0),$$ (4.1)

and

$$z = W(R), \quad \text{where} \quad W(R) \equiv f_z(R, 0) \equiv U_Z(R, 0).$$ (4.2)

The deformation of the middle plane into the middle *surface* is illustrated in Figure 3, below.
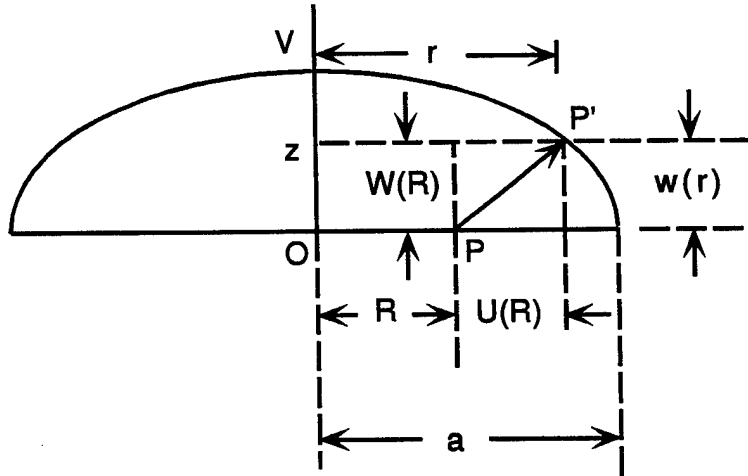
FIG. 3. Deformation of the Middle Plane $Z = 0$

We consider a circular membrane made of a material characterized by given values of Young's modulus E and Poisson's ratio ν. We assume that under a uniform pressure p the membrane is deformed to a new equilibrium configuration, illustrated in Figure 3, that is a solution of Hencky's equations [5]. This system of equations consists first of the following relations between the radial and circumferential strain tensor components and the displacement vector components:

$$\epsilon_R = \frac{dU}{dR} + \frac{1}{2}\left(\frac{dW}{dR}\right)^2,$$ (4.3)

5

$$\epsilon_\Theta = \frac{U}{R}, \tag{4.4}$$

where all variables are assumed to depend only upon the radial coordinate R of the reference configuration. The strain components are assumed to be linearly related to the second Piola-Kirchhoff stress components (see [3], pp. 465-466) by the following uniform, homogeneous, isotropic form of Hooke's Law:

$$S_R - \nu S_\Theta = E\,\epsilon_R, \tag{4.5}$$

$$S_\Theta - \nu S_R = E\,\epsilon_\Theta. \tag{4.6}$$

Finally, the stress components must satisfy the force equilibrium equations

$$S_\Theta = S_R + R\frac{dS_R}{dR} = \frac{d}{dR}(R\,S_R), \tag{4.7}$$

$$S_R\frac{dW}{dR} = -\frac{pR}{2h}, \tag{4.8}$$

representing equilibrium in the radial and lateral directions, respectively. We remark that Fichter [2] has recently suggested that (4.8) represents equilibrium in the lateral direction only for a *laterally applied* pressure load, and should be altered to include an additional term if the model is to represent a true pressure load (which would necessarily be *normal* to the deformed surface). Regardless of the merits of his suggestion, which at first sight appear to be well motivated physically, we adopt in this report the more familiar model using the equilibrium equation (4.8). We believe that Fichter's claim, if true, should be derived in a way that carefully distinguishes between variables defined on the reference and deformed configurations. Such a derivation has, to our knowledge, not been given.

Before going on to consider a particularly simple solution of these equations, we give details of the derivations of two useful differential equations that follow from (4.3)-(4.8). Differentiating (4.4), and using (4.3) and (4.4) in the result, we obtain

$$\frac{d\epsilon_\Theta}{dR} = \frac{1}{R}\frac{dU}{dR} - \frac{U}{R^2} = \frac{1}{R}\left[\epsilon_R - \frac{1}{2}\left(\frac{dW}{dR}\right)^2\right] - \frac{\epsilon_\Theta}{R},$$

which can be written as

$$R\frac{d\epsilon_\Theta}{dR} = \epsilon_R - \epsilon_\Theta - \frac{1}{2}\left(\frac{dW}{dR}\right)^2.$$

Multiplying this equation thru by E and using (4.5) and (4.6) to replace the strains in terms of the stresses yields

$$R\frac{d}{dR}(S_\Theta - \nu S_R) = S_R - \nu S_\Theta - S_\Theta + \nu S_R - \frac{E}{2}\left(\frac{dW}{dR}\right)^2.$$

On the right-hand side of the last equation, we use (4.7) to replace $S_R = S_\Theta - R(dS_R/dR)$, obtaining after some simplification:

$$R\frac{d}{dR}(S_\Theta + S_R) + \frac{E}{2}\left(\frac{dW}{dR}\right)^2 = 0, \tag{4.9}$$

which is Hencky's equation (4), and Campbell's equation (7). This can be written in terms of the pressure by using (4.8) to replace dW/dR, yielding

$$\frac{1}{R}S_R^2\frac{d}{dR}(S_\Theta + S_R) + \frac{E}{8}\frac{p^2}{h^2} = 0. \tag{4.10}$$

It is convenient to introduce at this point a dimensionless independent variable ρ defined by

$$\rho \equiv \frac{R}{a}, \tag{4.11}$$

as well as dimensionless displacement vector components $\widehat{U}$ and $\widehat{W}$, defined by

6

$$\widehat{U}(\rho) \equiv \frac{1}{a} U(a\rho), \qquad \widehat{W}(\rho) \equiv \frac{1}{a} W(a\rho), \tag{4.12}$$

and dimensionless stress components $\widehat{S}_R$ and $\widehat{S}_\Theta$, defined by

$$\widehat{S}_R(\rho) \equiv \frac{1}{E} S_R(a\rho), \qquad \widehat{S}_\Theta(\rho) \equiv \frac{1}{E} S_\Theta(a\rho). \tag{4.13}$$

We have departed somewhat from the Hencky-Campbell approach, as they define dimensionless stress components in terms of a factor k that is proportional to p. With our definitions, equations (4.3)-(4.8), (4.9), and (4.10) can be written in dimensionless form as

$$\epsilon_R = \frac{d\widehat{U}}{d\rho} + \frac{1}{2} \left(\frac{d\widehat{W}}{d\rho} \right)^2, \tag{4.14}$$

$$\epsilon_\Theta = \frac{\widehat{U}}{\rho}, \tag{4.15}$$

$$\widehat{S}_R - \nu \widehat{S}_\Theta = \epsilon_R, \tag{4.16}$$

$$\widehat{S}_\Theta - \nu \widehat{S}_R = \epsilon_\Theta, \tag{4.17}$$

$$\widehat{S}_\Theta = \widehat{S}_R + \rho \frac{d\widehat{S}_R}{d\rho} = \frac{d}{d\rho} (\rho \widehat{S}_R), \tag{4.18}$$

$$\widehat{S}_R \frac{d\widehat{W}}{d\rho} = -\frac{q}{2} \rho, \tag{4.19}$$

$$\rho \frac{d}{d\rho} (\widehat{S}_\Theta + \widehat{S}_R) + \frac{1}{2} \left(\frac{d\widehat{W}}{d\rho} \right)^2 = 0, \tag{4.20}$$

and

$$\frac{1}{\rho} \widehat{S}_R^2 \frac{d}{d\rho} (\widehat{S}_\Theta + \widehat{S}_R) + \frac{1}{8} q^2 = 0, \tag{4.21}$$

respectively, where

$$q \equiv \frac{pa}{Eh} \tag{4.22}$$

is a dimensionless constant proportional to the external pressure p.

V. EQUILIBRIUM CONFIGURATION OF AN UNPRESSURIZED CIRCULAR MEMBRANE

We consider here the solution of equations (4.14)-(4.19) when there is *no externally applied pressure*, which must include as one case the initially tensioned state assumed in Campbell's paper. With the exception of the radial coordinate on the deformed configuration, all variables in this special situation will carry a 0-subscript, hence the deformation equations corresponding to (4.1) and (4.2) will be written as

$$R = R_0 + U_0(R_0) \quad \text{and} \quad z_0 = W_0(R_0), \tag{5.1}$$

respectively. We also introduce, similarly to (4.11), a dimensionless radial coordinate ρ_0 defined by

7

$$\rho_0 \equiv \frac{R_0}{a}. \tag{5.2}$$

Thus, R_0 (or ρ_0) labels a point of the undeformed reference configuration, and R (or ρ) labels the point to which it may be deformed in the absence of external pressure.

It is convenient to again introduce dimensionless displacement vector and stress tensor components defined by

$$\widehat{U}_0(\rho_0) \equiv \frac{1}{a} U_0(a\rho_0), \qquad \widehat{W}_0(\rho_0) \equiv \frac{1}{a} W(a\rho_0), \tag{5.3}$$

and

$$\widehat{S}_{R0}(\rho_0) \equiv \frac{1}{E} S_{R0}(a\rho_0), \qquad \widehat{S}_{\Theta0}(\rho_0) \equiv \frac{1}{E} S_{\Theta0}(a\rho_0). \tag{5.4}$$

From (5.3), (4.11), (5.2) and (5.1), we obtain a dimensionless form of the equation of radial deformation:

$$\rho = \rho_0 + \widehat{U}_0(\rho_0). \tag{5.5}$$

The system of equations (4.14)-(4.19) with $p = 0$ (hence $q = 0$) can be written in terms of these dimensionless variables as

$$\epsilon_{R0} = \frac{d\widehat{U}_0}{d\rho_0} + \frac{1}{2}\left(\frac{d\widehat{W}_0}{d\rho_0}\right)^2, \tag{5.6}$$

$$\epsilon_{\Theta0} = \frac{\widehat{U}_0}{\rho_0}, \tag{5.7}$$

$$\widehat{S}_{R0} - \nu\,\widehat{S}_{\Theta0} = \epsilon_{R0}, \tag{5.8}$$

$$\widehat{S}_{\Theta0} - \nu\,\widehat{S}_{R0} = \epsilon_{\Theta0}, \tag{5.9}$$

$$\widehat{S}_{\Theta0} = \widehat{S}_{R0} + \rho_0\,\frac{d\widehat{S}_{R0}}{d\rho_0} = \frac{d}{d\rho_0}\left(\rho_0\,\widehat{S}_{R0}\right), \tag{5.10}$$

$$\widehat{S}_{R0}\,\frac{d\widehat{W}_0}{d\rho_0} = 0, \tag{5.11}$$

It follows immediately from (5.11) that either $\widehat{S}_{R0}$ is zero, or $\widehat{W}_0(\rho_0)$ is a constant, or both of these conditions hold. It is easy to see that if $\widehat{S}_{R0} = 0$, then all dependent variables except $\widehat{W}_0$ vanish, and $\widehat{W}_0$ is again relegated to some constant value by equation (5.6).

The remaining possibility, then, is that $\widehat{W}_0(\rho_0)$ is constant, but $\widehat{S}_{R0} \neq 0$. Under these conditions, the lateral equilibrium equation (5.11) is identically satisfied, and equation (5.6) for the radial strain reduces to

$$\epsilon_{R0} = \frac{d\widehat{U}_0}{d\rho_0}, \tag{5.12}$$

hence the system we must solve consists of equations (5.7), (5.8), (5.9), (5.10), and (5.12), subject to the requirement that all functions be regular (i.e., be defined for all values of ρ_0). We begin by using (5.10) to replace $\widehat{S}_{\Theta0}$ in the left-hand sides of (5.8) and (5.9), and using (5.7) and (5.12) in the right-hand sides of the same two equations, to write them as

$$(1 - \nu)\,\widehat{S}_{R0} - \nu\,\rho_0\,\frac{dS_{R0}}{d\rho_0} = \frac{d\widehat{U}_0}{d\rho_0},$$

and

8

$$(1 - \nu)\,\widehat{S}_{R0} + \rho_0\,\frac{d\widehat{S}_{R0}}{d\rho_0} = \frac{\widehat{U}_0}{\rho_0}.$$

Subtracting the first of these two equations from the second, we obtain

$$(1 + \nu)\,\rho_0\,\frac{d\widehat{S}_{R0}}{d\rho_0} = \Big(\frac{\widehat{U}_0}{\rho_0} - \frac{d\widehat{U}_0}{d\rho_0}\Big),$$

which can be rewritten as

$$\frac{d\widehat{S}_{R0}}{d\rho_0} = -\frac{1}{1 + \nu}\Big(\frac{1}{\rho_0}\frac{d\widehat{U}_0}{d\rho_0} - \frac{\widehat{U}_0}{\rho_0^2}\Big) \equiv -\frac{1}{1 + \nu}\frac{d}{d\rho_0}\Big(\frac{\widehat{U}_0}{\rho_0}\Big).$$

This integrates immediately to obtain

$$\widehat{S}_{R0} = c_1 - \Big(\frac{1}{1 + \nu}\Big)\frac{\widehat{U}_0}{\rho_0}, \tag{5.13}$$

where c_1 is an arbitrary integration constant. Substitution of (5.13) and (4.4) in (4.6) yields

$$\widehat{S}_{\Theta 0} = c_1\,\nu + \Big(\frac{1}{1 + \nu}\Big)\frac{\widehat{U}_0}{\rho_0}. \tag{5.14}$$

Finally, substitution of (5.13), (5.14) and (5.12) in (5.8) yields a differential equation for $\widehat{U}_0(\rho_0)$:

$$c_1 - \Big(\frac{1}{1 + \nu}\Big)\frac{\widehat{U}_0}{\rho_0} - \nu\Big[c_1\,\nu + \Big(\frac{1}{1 + \nu}\Big)\frac{\widehat{U}_0}{\rho_0}\Big] = \frac{d\widehat{U}_0}{d\rho_0},$$

which can be rearranged to write it as

$$\frac{d}{d\rho_0}(\rho_0\,\widehat{U}_0) = c_1\,(1 - \nu^2)\,\rho_0,$$

which easily integrates to obtain

$$\widehat{U}_0(\rho_0) = c_1\,\frac{1 - \nu^2}{2}\,\rho_0 + \frac{c_2}{\rho_0}.$$

In this expression, the arbitrary integration constant c_2 must be set equal to zero in order for $\widehat{U}_0$ to be regular at $\rho_0 = 0$, hence the general solution for $\widehat{U}_0$ reduces to

$$\widehat{U}_0(\rho_0) = c_1\,\frac{1 - \nu^2}{2}\,\rho_0. \tag{5.15}$$

Substitution of this result in (5.6) and (5.7), recalling that $\widehat{W}_0$ is constant, yields

$$\epsilon_{R0} = \epsilon_{\Theta 0} = c_1\,\frac{1 - \nu^2}{2} \equiv \epsilon, \tag{5.16}$$

i.e., the two strain components are equal to the same constant value, which we denote by ϵ. From (5.8) and (5.9) it then follows that the two stress components are also equal and constant throughout the membrane:

$$\widehat{S}_{R0} = \widehat{S}_{\Theta 0} = \Big(\frac{1}{1 - \nu}\Big)\epsilon \equiv \widehat{S}. \tag{5.17}$$

In terms of the constant strain ϵ, the radial displacement (5.15) is given by the linear relation

$$\widehat{U}_0(\rho_0) = \epsilon\,\rho_0 \quad \Rightarrow \quad \widehat{U}_0(1) = \epsilon. \tag{5.18}$$

Thus, Campbell's configuration of initial tension σ (which corresponds to $S \equiv E\,\widehat{S}$ in the preceding development) is *equivalent* to a configuration in which each point has suffered a linear radial displacement from its unstrained reference configuration. The radial deformation (5.5) is found from (5.18) and (5.16) to have the simple form

$$\rho = \rho_0(1 + \epsilon), \tag{5.19}$$

while the lateral deformation is taken to be

$$z_0 = 0, \tag{5.20}$$

assuming the constant lateral displacement to be zero, i.e., $\widehat{W}_0(\rho_0) = 0$. Since $\widehat{W}_0(\rho_0)$ is constant, this will be true if, for example, the membrane remains in contact with the hoop edge at $R_0 = a$ during the radial displacement.

VI. CAMPBELL'S PROBLEM

We consider now a membrane which has suffered a purely radial displacement of its edge. As shown in the previous Section, this introduces an initial uniform dimensionless stress $\widehat{S}$ and corresponding strain ϵ, related by (5.17). Body points of the middle plane of this *pre-strained membrane* are labeled by the radial coordinate R, as in the previous Section. The membrane is subsequently clamped along the circle $R = a$, and an external uniform pressure is applied to points of the disk $R \leq a$. In terms of dimensionless variables defined at points of this pressurized part of the pre-strained membrane labeled by the dimensionless radial variable $\rho = R/a$, the Hencky-Campbell equations can be written as

$$\epsilon_R = \epsilon + \frac{d\widehat{U}}{d\rho} + \frac{1}{2}\left(\frac{d\widehat{W}}{d\rho}\right)^2, \tag{6.1}$$

$$\epsilon_\Theta = \epsilon + \frac{\widehat{U}}{\rho}, \tag{6.2}$$

$$\widehat{S}_R - \nu\widehat{S}_\Theta = \epsilon_R, \tag{6.3}$$

$$\widehat{S}_\Theta - \nu\widehat{S}_R = \epsilon_\Theta, \tag{6.4}$$

$$\widehat{S}_\Theta = \widehat{S}_R + \rho\frac{d}{d\rho}(\widehat{S}_R) = \frac{d}{d\rho}(\rho\widehat{S}_R), \tag{6.5}$$

$$\widehat{S}_R\frac{d\widehat{W}}{d\rho} = -\frac{q}{2}\rho, \tag{6.6}$$

$$\rho\frac{d}{d\rho}(\widehat{S}_\Theta + \widehat{S}_R) + \frac{1}{2}\left(\frac{d\widehat{W}}{d\rho}\right)^2 = 0, \tag{6.7}$$

and

$$\frac{1}{\rho}\widehat{S}_R^2\frac{d}{d\rho}(\widehat{S}_\Theta + \widehat{S}_R) + \frac{1}{8}q^2 = 0, \tag{6.8}$$

We remark that the stress and strain components in these equations are the *total* stresses and strains, not the *incremental* stresses and strains used by Campbell. The non-zero pre-strain is accounted for in equations (6.1) and (6.2), which are modifications of Hencky's equations (4.14) and (4.15) needed to assure that the total stress and strain in the membrane reduce to the pre-stress and pre-strain when the displacement components $\widehat{U}$ and $\widehat{W}$ vanish (corresponding to a reduction of the external pressure to zero). Since the membrane is clamped along the circle $R = a$, corresponding to $\rho = 1$, the appropriate boundary conditions to be applied are

$$\widehat{U}(1) = 0, \quad \text{and} \quad \widehat{W}(1) = 0. \tag{6.9}$$

Similarly to Hencky and Campbell, we begin by assuming an even power series solution for the dimensionless total stress component $\widehat{S}_R$ of the form

$$\widehat{S}_R = b_0\left(1 + \sum_{n=1} b_{2n}\rho^{2n}\right), \tag{6.10}$$

where the coefficients b_{2n}, $n = 1, 2, 3, \ldots$, are dimensionless constants. Substitution of this expression in (6.5) yields

$$\widehat{S}_\Theta = \frac{d}{d\rho}(\rho\widehat{S}_R) = b_0\left[1 + \sum_{n=1}(2n+1)b_{2n}\rho^{2n}\right]. \tag{6.11}$$

10

From the last two equations we obtain

$$\widehat{S}_R + \widehat{S}_\Theta = 2\,b_0 \left[1 + \sum_{n=1}(n+1)b_{2n}\rho^{2n}\right],$$

hence

$$\frac{1}{\rho}\frac{d}{d\rho}(\widehat{S}_R + \widehat{S}_\Theta) = 4\,b_0 \sum_{n=1} n(n+1)b_{2n}\rho^{2n-2},$$

This is substituted, together with (6.10), into (6.8) to obtain

$$4\,b_0^3 \left(1 + \sum_{n=1} b_{2n}\rho^{2n}\right)^2 \cdot \sum_{n=1} n(n+1)b_{2n}\rho^{2n-2} + \frac{1}{8}q^2 = 0,$$

which we rewrite as

$$\left(1 + \sum_{n=1} b_{2n}\rho^{2n}\right)^2 \cdot \sum_{n=1} \frac{n(n+1)}{2}b_{2n}\rho^{2n-2} + \mathcal{B}^2 = 0, \qquad (6.12)$$

where we have introduced a new dimensionless constant $\mathcal{B}$ defined by

$$\mathcal{B} \equiv \frac{1}{8}\frac{q}{b_0^{3/2}} \quad \Rightarrow \quad b_0 = \frac{1}{4}\left(\frac{q}{\mathcal{B}}\right)^{2/3}. \qquad (6.13)$$

The expanded form of (6.12) is

$$\left(1 + b_2\rho^2 + b_4\rho^4 + b_6\rho^6 + \dots\right)^2 \left(b_2 + 3b_4\rho^2 + 6b_6\rho^4 + 10b_8\rho^6 + \dots\right) + \mathcal{B}^2 = 0. \qquad (6.14)$$

This is used to obtain all coefficients b_{2n}, $n \geq 1$, in terms of $\mathcal{B}$, by computing the products of the three infinite series, and equating to zero each coefficient of different powers of ρ. We have made use of the *Mathematica** software system to determine that each of these coefficients has the form

$$b_{2n} = -\beta_{2n}\,\mathcal{B}^{2n}, \qquad (6.15)$$

where the purely numerical coefficients β_{2n} for $n = 1$ to $n = 11$ are given by

$$\beta_2 = 1, \quad \beta_4 = \frac{2}{3}, \quad \beta_6 = \frac{13}{18}, \quad \beta_8 = \frac{17}{18}, \quad \beta_{10} = \frac{37}{27},$$

$$\beta_{12} = \frac{1205}{567}, \quad \beta_{14} = \frac{219241}{63504}, \quad \beta_{16} = \frac{6634069}{1143072},$$

$$\beta_{18} = \frac{51523763}{5143824}, \quad \beta_{20} = \frac{998796305}{56582064}, \quad \beta_{22} = \frac{118156790413}{3734416224}. \qquad (6.16)$$

Now, substituting (6.2) in the right-hand side of (6.4), and evaluating the result at the edge boundary $\rho = 1$, yields

$$b_0\left(1 + 3b_2 + 5b_4 + 7b_6 + 9b_8 + \dots\right) - \nu b_0\left(1 + b_2 + b_4 + b_6 + b_8 + \dots\right) = \epsilon + \widehat{U}(1) = \epsilon,$$

where we applied the first boundary condition (6.9). This can be rewritten, after collecting like terms on the left-hand side, as

$$\left[(1 - \nu) + (3 - \nu)b_2 + (5 - \nu)b_4 + (7 - \nu)b_6 + (9 - \nu)b_8 + \dots\right] - \frac{\epsilon}{b_0} = 0. \qquad (6.17)$$

Since all the coefficients have been expressed in terms of $\mathcal{B}$, or equivalently, in terms of b_0, the left-hand side of (6.17) defines a function whose independent variable is b_0. According to (6.17), the remaining constant b_0 must be

---

determined as a *zero* of this function. This can be done by standard numerical methods, e.g., the bisection method given in [8] is quite satisfactory for our purposes.

Once the coefficient b_0 has been determined, the dimensionless stress components are given by the even-order power series (6.10) and (6.11), while $\widehat{U}(\rho)$ is given, according to (6.2) and (6.4), by the odd-order series

$$\widehat{U}(\rho) = \rho\,(\widehat{S}_\Theta - \nu\widehat{S}_R) - \rho\,\epsilon = b_0\,\rho\,[\,(1-\nu) + \sum_{n=1}(2n+1-\nu)\,b_{2n}\rho^{2n}\,] - \rho\,\epsilon. \tag{6.18}$$

Similarly, the two strain components are obtained by substituting the appropriate series into (6.3) and (6.4), to obtain

$$\epsilon_R = \widehat{S}_R - \nu\widehat{S}_\Theta = b_0\,\{\,(1-\nu) + \sum_{n=1}[1-\nu(2n+1)]\,b_{2n}\rho^{2n}\,), \tag{6.19}$$

and

$$\epsilon_\Theta = \widehat{S}_\Theta - \nu\widehat{S}_R = b_0\,\{\,(1-\nu) + \sum_{n=1}(2n+1-\nu)\,b_{2n}\rho^{2n}\,). \tag{6.20}$$

The remaining dimensionless variable $\widehat{W}(\rho)$ can be determined by assuming an even-order power series of the form

$$\widehat{W}(\rho) = \sum_{n=0}\widehat{w}_{2n}\,\rho^{2n}, \tag{6.21}$$

the derivative of which is

$$\frac{d\widehat{W}}{d\rho} = 2\sum_{n=0}n\,\widehat{w}_{2n}\,\rho^{2n-1}. \tag{6.22}$$

Substitution of (6.22) and (6.10) in (6.6) yields

$$2b_0\,(1 + \sum_{n=1}b_{2n}\rho^{2n}\,)\sum_{n=0}n\,\widehat{w}_{2n}\,\rho^{2n-1} + \frac{q}{2}\,\rho = 0,$$

or

$$(1 + \sum_{n=1}b_{2n}\rho^{2n}\,)\sum_{n=0}n\,c_{2n}\,\rho^{2n-1} + \rho = 0. \tag{6.23}$$

In the last line we have defined new coefficients c_{2n} such that $\widehat{w}_{2n} \equiv \mathcal{C}\,c_{2n}$, $n \geq 1$, where

$$\mathcal{C} \equiv \frac{1}{4}\frac{q}{b_0} \tag{6.24}$$

is another dimensionless constant. Expanding the product of the two infinite series in (6.23), replacing each b_{2n} in terms of $\mathcal{B}$, and then equating coefficients of like powers of ρ to zero we find, again making extensive use of the *Mathematica* system, that

$$c_{2n} = -\gamma_{2n}\,\mathcal{B}^{2n-2}, \tag{6.25}$$

where the purely numerical coefficients γ_{2n} for $n=1$ to $n=10$ are given by

$$\gamma_2 = 1, \quad \gamma_4 = \frac{1}{2}, \quad \gamma_6 = \frac{5}{9}, \quad \gamma_8 = \frac{55}{72}, \quad \gamma_{10} = \frac{7}{6},$$

$$\gamma_{12} = \frac{205}{108}, \quad \gamma_{14} = \frac{17051}{5292}, \quad \gamma_{16} = \frac{2864485}{508032},$$

$$\gamma_{18} = \frac{741805}{10287648}, \quad \gamma_{20} = \frac{16659221}{5143824}. \tag{6.26}$$

The remaining coefficient $\widehat{w}_0$ is determined by the second boundary condition of (6.9), viz., $\widehat{W}(1) = 0$, which yields from (6.21):

$$0 = \widehat{w}_0 + \mathcal{C}\sum_{n=1}c_{2n} \quad \Rightarrow \quad \widehat{w}_0 = -\mathcal{C}\sum_{n=1}c_{2n}. \tag{6.27}$$

Power series expressions for each of the dimensionless variables are now completely determined. Each of these must be truncated after a finite number of terms, determined by the error acceptable by the user.

12

VII. THE EQUATION OF THE "TRUE" MIDDLE SURFACE

The solutions $U(R)$ and $W(R)$ can be substituted in equations (4.1) and (4.2) to obtain the deformation mappings:

$$r = F(R) = R + U(R), \quad \text{and} \quad z = W(R). \tag{7.1}$$

They can be interpreted as *parametric equations* of the middle surface, with parameter R. The second equation of (7.1) defines the surface of *lateral displacements* of the body points with radial coordinates R. The graph of this equation is frequently identified with the middle surface, but it does *not* define the *true* middle surface (this observation has been emphasized in a recent AIAA Proceedings paper [4]). Points on the middle surface are coordinatized by (r, z), not (R, z), hence the equation of the middle surface must relate the lateral displacement z to the radial coordinate r of the point in the deformed configuration that was *originally* at R. Thus, it must take into account the radial displacement $U(R)$ as well. As can be seen in Figure 3, the true middle surface should be graphed by plotting the lateral displacement $z = W(R)$ versus the point of the middle plane with coordinate $r = R + U(R)$ (*not* against the point with coordinate R).

For some purposes it is convenient to actually eliminate the parameter R between the two relations in (7.1). We first introduce on the deformed configuration a dimensionless radial variable ξ, defined by

$$\xi = \frac{r}{a}, \tag{7.2}$$

so that, recalling the definition $\rho = R/a$, hence $R = a\rho$, we can evaluate the two relations in (7.1) at $R = a\rho$ to obtain

$$\xi = \frac{1}{a} F(R) = \frac{1}{a} F(a\rho) \equiv \widehat{F}(\rho) = \rho + \widehat{U}(\rho), \quad \text{and} \quad z = W(R) = W(a\rho) = a\widehat{W}(\rho), \tag{7.3}$$

where we recall that $U(a\rho) = a\widehat{U}(\rho)$. One can, in principle, solve the first of these relations to obtain ρ as a function of ξ, i.e.,

$$\rho = \widehat{F}^{-1}(\xi), \tag{7.4}$$

which can then be substituted into the second relation to obtain

$$z = W(R) = a\widehat{W}(\widehat{F}^{-1}(\xi)) \equiv a\widehat{w}(\xi) = a\widehat{w}(r/a) \equiv w(r). \tag{7.5}$$

The final equality is, formally, the equation of the true middle surface.

Of course, it is difficult, if not impossible, to determine the *exact* relation (7.4). However, such a relation can be found to any desired accuracy, as follows. We substitute the infinite series (6.18) for $\widehat{U}(\rho)$ into the first relation in (7.3), and write the result as

$$\begin{aligned}
\xi = \widehat{F}(\rho) &= [(1 - \epsilon) + b_0(1 - \nu)]\rho + b_0 b_2(3 - \nu)\rho^3 + b_0 b_4(5 - \nu)\rho^5 + \dots, \\
&\equiv d_1\rho + d_3\rho^3 + d_5\rho^5 + \dots.
\end{aligned} \tag{7.6}$$

We then express the variable ρ as an infinite series in ξ, viz.,

$$\rho = \widehat{F}^{-1}(\xi) = f_1\xi + f_3\xi^3 + f_5\xi^5 + \dots, \tag{7.7}$$

where the f_{2n+1} are determined by substituting (7.7) for ρ into (7.6), and equating like powers of ξ in the result. For example, we find in this way

$$f_1 = \frac{1}{d_1}, \quad f_3 = -\frac{d_3}{d_1^4}, \quad f_5 = \frac{3d_3^2 - d_1 d_5}{d_1^7}, \quad f_7 = \frac{8d_1 d_3 d_5 - 12d_3^3 - d_1^2 d_7}{d_1^{10}}, \tag{7.8}$$

again making use of the *Mathematica* system. In practice, the coefficients of the highest order terms retained in the power series (7.6) and (7.7) are chosen to satisfy the boundary condition on the circle $\rho = 1$, viz., $\widehat{U}(1) = 0$, which in turn requires that $\xi = 1$ when $\rho = 1$. For example, we find that for pre-strains and pressures relevant to the laboratory membrane, ξ is well-approximated by the truncated series

$$\xi = d_1\rho + d_3\rho^3 + d_{55}\rho^5, \quad d_{55} \equiv 1 - d_1 - d_3, \tag{7.9}$$

13

while ρ can be approximated by

$$\rho = f_1 \xi + f_3 \xi^3 + f_{55} \xi^5, \qquad f_{55} \equiv 1 - f_1 - f_3. \tag{7.10}$$

Once the series (7.7) for ρ is determined to the desired accuracy, the result can be substituted for $\rho = \widehat{F}^{-1}(\xi)$ in the power series representation (6.21) of $\widehat{W}(\rho)$, yielding according to (7.5) a series solution for the equation of the true middle surface:

$$w(r) = a \left\{ \widehat{w}_0 + \mathcal{C} \sum_{n=1} c_{2n} \left[\widehat{F}^{-1}(r/a) \right]^{2n} \right\}, \tag{7.11}$$

or, in dimensionless form:

$$\widehat{w}(\xi) = \widehat{w}_0 + \mathcal{C} \sum_{n=1} c_{2n} \left[\widehat{F}^{-1}(\xi) \right]^{2n}, \tag{7.12}$$

and we note that since $\widehat{F}^{-1}(1) = 1$, we have $\widehat{w}(1) = 0$, as required. In Figure 4 we show a rather extreme case (zero pre-strain and an f-number of 2) of the difference between the true surface and the surface of lateral displacements. For pre-strains of as little as 0.1% and high f-numbers, say $f/8$, the difference is, however, negligibly small (on the order of tenths of a wavelength).
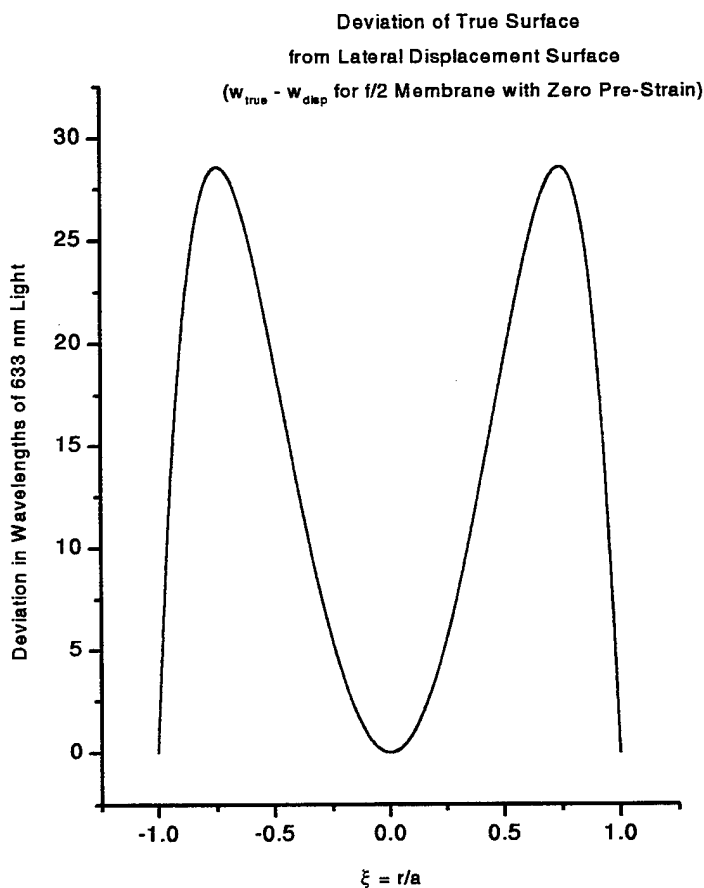

Deviation of True Surface

from Lateral Displacement Surface

($W_{true} - W_{disp}$ for f/2 Membrane with Zero Pre-Strain)

FIG. 4. Deviation of True Surface from Surface of Lateral Displacements ($f/2$ Membrane)

VIII. THE MEMBRANE SURFACE AS A FUNCTION OF *F*-NUMBER

Referring to Figure 3, we note that for $r \ll a$, i.e., near the vertex of the membrane where $r = 0$, the equation of the surface is approximated by the first two terms of (7.11), viz.,

$$w(r) \approx a \left[\widehat{w}_0 + C c_2 f_1^2 \left(\frac{r}{a} \right)^2 \right] = w_0 - \frac{C f_1^2}{a} r^2, \tag{8.1}$$

where we replaced $c_2 = -\gamma_2 = -1$ in the final equality. This is recognized to be the equation of a paraboloid with origin at O, having a focal length f given by

$$f = \frac{a}{4 C f_1^2} = \frac{a d_1^2}{4 C}, \tag{8.2}$$

where the final equality follows from the first relation in (7.8). In all that follows, we consider this "paraxial" focal length to be the focal length of the membrane. It is convenient to replace f by the membrane *f*-number, $f/\#$, defined by

$$f/\# = \frac{f}{2a}, \tag{8.3}$$

where $2a$ is the membrane diameter. From (8.2) and (8.3) it then follows that

$$f/\# = \frac{d_1^2}{8 C}. \tag{8.4}$$

which relates the *f*-number to the mechanical properties of the membrane (recall that d_1 depends on both ϵ and ν according to (7.6), while C depends on $q = pa/Eh$ according to (6.24) and (4.22)).

In order to determine the equation of the membrane surface for a given *f*-number $f/\#$, and given values of ϵ and ν, we begin by noting from (8.4) that C must in this case be given by

$$C = \frac{d_1^2}{8 f/\#} = \frac{[(1 - \epsilon) + b_0(1 - \nu)]^2}{8 f/\#}, \tag{8.5}$$

where the last expression follows from (7.6). From the definition (6.24) we obtain the following relation between C, b_0, and the variable q:

$$q = 4 b_0 C. \tag{8.6}$$

Substitution of this expression into (6.13) yields

$$\mathcal{B} = \frac{C}{2\sqrt{b_0}}. \tag{8.7}$$

These expressions for C and $\mathcal{B}$ as functions of b_0 are now used in (6.17), to determine b_0 as a solution of

$$[(1 - \nu) + (3 - \nu)b_2 + (5 - \nu)b_4 + (7 - \nu)b_6 + (9 - \nu)b_8 + \ldots] - \frac{\epsilon}{b_0} = 0, \tag{8.8}$$

for a given value of the pre-strain ϵ. Once b_0 is determined, the coefficients in the power series for the displacement components and other variables can be computed. The pressure for this value of b_0, and the given values of the parameters ϵ, ν, and $f/\#$, is found from the definition (4.22):

$$p = q \frac{Eh}{a}, \tag{8.9}$$

after q has been computed from (8.6). The maximum displacement is

$$w_0 = a \widehat{w}_0, \tag{8.10}$$

where $\widehat{w}_0$ has been computed according to (6.27).

15

IX. ESTIMATION OF THE PRE-STRAIN AS A FUNCTION OF F-NUMBER

Suppose that at a given pressure p the membrane is characterized as having a particular f-number $f/\#$. The amount of pre-strain ϵ for these values of p and $f/\#$ is difficult to measure directly, but can be calculated as follows. From (8.5), (8.6), and (4.22), we have

$$p = \frac{Eh}{a} b_0 \frac{[1 + b_0 (1 - \nu) - \epsilon]^2}{2 f/\#},$$ (9.1)

which can be solved for ϵ as a function of the known parameters, and the unknown coefficient b_0:

$$\epsilon = 1 + b_0 (1 - \nu) - \sqrt{\frac{2 f/\#}{b_0} \frac{a}{Eh}} \sqrt{p}.$$ (9.2)

Since p is known, we can compute q from (4.22), and then from (6.24) and (6.13) get C and B as functions of the unknown coefficient b_0:

$$C = \frac{q}{4 b_0}, \qquad B = \frac{q}{8 b_0^{3/2}}.$$ (9.3)

These expressions for ϵ and B as functions of b_0 are now substituted in (8.8), which is solved for b_0. This value of b_0 can then be used in (9.2) to obtain the desired estimate of the pre-strain ϵ at the given values of p and $f/\#$.

We also note that for $\epsilon/[1 + b_0 (1 - \nu)] << 1$, we obtain from (9.1) a linear approximation of p as a function of ϵ:

$$p \approx \frac{Eh}{a} \frac{b_0}{2 f/\#} [1 + b_0 (1 - \nu)]^2 - \frac{Eh}{a} \frac{b_0}{f/\#} [1 + b_0 (1 - \nu)] \epsilon \equiv p_0 - m \epsilon,$$ (9.4)

where the p-intercept and slope m are given by

$$p_0 = \frac{Eh}{a} \frac{b_0}{2 f/\#} [1 + b_0 (1 - \nu)]^2, \quad \text{and} \quad m = \frac{Eh}{a} \frac{b_0}{f/\#} [1 + b_0 (1 - \nu)].$$ (9.5)

The approximation (9.4) yields the following linear approximation for the pre-strain as a function of pressure, for a given $f/\#$:

$$\epsilon \approx \frac{p_0 - p}{m}.$$ (9.6)

X. ESTIMATION OF THE PRE-STRAIN AS A FUNCTION OF MAXIMUM LATERAL DISPLACEMENT

It has been found useful to have at least an approximate solution of the following problem: what pre-strain ϵ is required to obtain a desired maximum lateral displacement of the membrane for a given pressure p? We note that from (6.21) and (6.27) we have the following expression for the maximum displacement W_0:

$$W(0) = W_0 = a \widehat{w}_0 = -a C \sum_{n=1} c_{2n},$$

or, using (6.25):

$$W_0 = a C (\gamma_2 + \gamma_4 B^2 + \gamma_6 B^4 + \gamma_8 B^6 + \ldots + \gamma_{20} B^{18}),$$

where we recall from (6.26) that γ_{2n} is the numerical coefficient of B^{2n-2} in each series coefficient c_{2n}, e.g., $\gamma_2 = 1$, $\gamma_4 = 1/2$, $\gamma_6 = 5/9$, and $\gamma_8 = 55/72$. Using (6.24) to replace C yields

$$W_0 = \frac{aq}{4} \frac{1}{b_0} (\gamma_2 + \gamma_4 B^2 + \gamma_6 B^4 + \gamma_8 B^6 + \ldots + \gamma_{20} B^{18}).$$ (10.1)

The coefficient $\mathcal{B}$ depends, in general, on b_0 and q according to its definition (6.13), and we recall that b_0 is determined for a given q, ν, and ϵ by solving (6.17).

However, for $\epsilon = 0$, equation (6.17) reduces to

$$1 - \nu) + (3 - \nu)b_2 + (5 - \nu)b_4 + (7 - \nu)b_6 + (9 - \nu)b_8 + \ldots = 0. \tag{10.2}$$

which can be solved for $\mathcal{B}$ without regard for q, requiring only a given value for ν [the coefficients b_{2n}, $n \geq 1$, depend only on $\mathcal{B}$, according to (6.15)]. Denoting by $\mathcal{B}_0$ the value of $\mathcal{B}$ corresponding to $\epsilon = 0$, we have from (6.13):

$$b_{00} = \frac{1}{4}\left(\frac{q}{\mathcal{B}_0}\right)^{2/3}, \tag{10.3}$$

for the value of b_0 when $\epsilon = 0$. This can be substituted for b_0 in (10.1) to obtain the maximum displacement with zero pre-strain:

$$W_0 = a\,q^{1/3}\mathcal{B}_0^{2/3}\left(\gamma_2 + \gamma_4\mathcal{B}^2 + \gamma_6\mathcal{B}^4 + \gamma_8\mathcal{B}^6 + \ldots + \gamma_{20}\mathcal{B}^{18}\right) \equiv \mathcal{K}\,a\,q^{1/3}, \tag{10.4}$$

where we have introduced a new constant $\mathcal{K}$ defined by

$$\mathcal{K} \equiv \mathcal{B}_0^{2/3}\left(\gamma_2 + \gamma_4\mathcal{B}^2 + \gamma_6\mathcal{B}^4 + \gamma_8\mathcal{B}^6 + \ldots + \gamma_{20}\mathcal{B}^{18}\right). \tag{10.5}$$

We remark that our equation (10.4) is equivalent to Campbell's equation (25), where $\mathcal{K} = 0.653$ corresponds to his use of a Poisson's ratio $\nu = 0.3$. We have verified this value of $\mathcal{K}$ with our computations, and find that when we increase ν to $\nu = 0.4$, the value decreases to $\mathcal{K} = 0.626$. Once this constant has been determined for a given value of ν, we can solve (10.4) for the pressure:

$$p_0 = \frac{Eh}{a}\left(\frac{W_0}{\mathcal{K}a}\right)^3, \tag{10.6}$$

which is the pressure required to produce a desired maximum displacement W_0 when there is zero pre-strain.

Now, in the opposite limit of *large* pre-strain, we find numerically that the parameter $\mathcal{B}$ tends to a number much less than 1, hence the terms in (10.1) involving $\mathcal{B}$ can be neglected to yield the approximation

$$W_0 = \frac{aq}{4}\frac{1}{b_{0\infty}}, \tag{10.7}$$

where we denote by $b_{0\infty}$ the value of b_0 for large values of ϵ. In the same approximation, since the coefficients b_{2n}, $n \geq 1$, are proportional to powers of $\mathcal{B}$, the determining equation (6.17) reduces to simply

$$1 - \nu - \frac{\epsilon}{b_{0\infty}} = 0 \quad \Rightarrow \quad b_{0\infty} = \frac{\epsilon}{1 - \nu}. \tag{10.8}$$

Substituting (4.22), and this expression for $b_{0\infty}$, in (10.7) yields the following expression for the pressure under large pre-strain conditions:

$$p_\infty = 4\frac{Eh}{a}\frac{W_0}{1 - \nu}\epsilon. \tag{10.9}$$

The curve of pressure versus pre-strain for a given value of W_0 has been found to be well-approximated by the linear function obtained from the sum of the two extreme cases (10.6) and (10.9):

$$p(\epsilon) \approx p_0 + m\,\epsilon, \tag{10.10}$$

where the p-intercept p_0, and slope m, are given by

$$p_0 = \frac{Eh}{a}\left(\frac{W_0}{\mathcal{K}a}\right)^3 \quad \text{and} \quad m = 4\frac{Eh}{a}\frac{W_0}{1 - \nu}, \tag{10.11}$$

respectively. Thus, by measuring the pressure p required to produce a (measured) maximum displacement W_0, we can invert (10.10) to obtain an estimate for the amount of initial strain existing in the membrane:

$$\epsilon \approx \frac{p - p_0}{m}. \tag{10.12}$$

Unfortunately, a precise direct measurement of W_0 is also difficult to obtain.

XI. COMPARISONS WITH REFERENCE SURFACES

In Figure 5 we have illustrated again the displacement of point P of an initially flat membrane to point P' of its equilibrium deformed configuration. We have also shown there a sphere of radius R_c with center at C, which has been chosen to coincide with the membrane at the vertex V and along the circular membrane edge $r = a$. The equation of the middle surface of the deformed membrane, in a frame with origin at O, is given by (7.5), i.e.,

$$z = w(r). \tag{11.1}$$

The center O of the middle plane $Z = 0$ is displaced under the deformation to the vertex V of the membrane, which has coordinates $(0, w_0)$, where $w_0 \equiv w(0) = W(0) = W_0$ is the maximum lateral displacement.
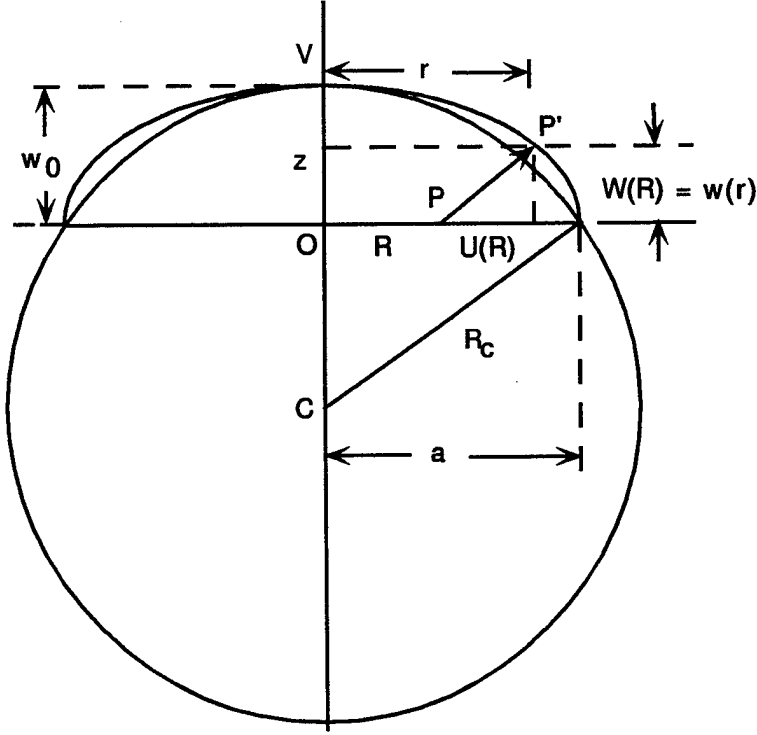

FIG. 5. Geometry of Reference Sphere

In Figure 5, a point with Cartesian coordinates $\{x, y, z\}$ in the frame with origin at O has coordinates $\{x, y, \tilde{z}\}$ in a frame with origin at the vertex V. The two axial coordinates are related by a translation through the maximum displacement w_0, i.e.,

$$\tilde{z} = z - w_0, \tag{11.2}$$

which assures that the vertex V defined by $\tilde{z} = 0$ corresponds to $z = w_0$ with respect to O. The equation of the membrane surface in a frame with origin at V is thus

$$\tilde{z} = w(r) - w_0. \tag{11.3}$$

In this coordinate system, the equation of a *paraboloid* with focal length f_P has the particularly simple form

$$\tilde{z}_P = -\frac{1}{4f_P} r^2, \tag{11.4}$$

while points on the surface of the upper hemisphere of a *sphere* of arbitrary radius R_c satisfy the equation

$$\tilde{z}_S = -R_c + \sqrt{R_c^2 - r^2}, \tag{11.5}$$

which is easily derived from the geometry of Figure 5. We note that for $r \ll R_c$ (i.e., near the vertex V), the equation of the sphere is approximated by

18

$$\tilde{z}_S \approx -\frac{1}{2R_c}r^2, \tag{11.6}$$

which we obtained by keeping only the first two terms in the binomial expansion of the square root function in (11.5). According to (11.4), this represents a paraboloid of focal length $f_S = R_c/2$. Translating back to the coordinate system with origin at the membrane center O, the equations for spherical and paraboloidal surfaces passing through the vertex V are given by

$$z_S = w_S(r) = w_0 - R_c + \sqrt{R_c^2 - r^2}, \tag{11.7}$$

$$\approx w_0 - \frac{1}{2R_c}r^2, \qquad r \ll R_c, \tag{11.8}$$

and

$$z_P = w_P(r) = w_0 - \frac{1}{4f_P}r^2, \tag{11.9}$$

where the approximation (11.8) holds near the vertex.

We note that the plane $z = 0$ intersects the membrane surface in a circle of radius a, which suggests choosing as a reference sphere one obtained by requiring that the plane $z = 0$ also cut the spherical surface in a circle of radius $r = a$, as shown in Figure 5. From (11.7) it follows that the maximum displacement w_0, the membrane radius a, and the radius R_c of the sphere, must then satisfy the condition

$$w_0 = R_c - \sqrt{R_c^2 - a^2}. \tag{11.10}$$

This can be solved for the radius of curvature, to obtain

$$R_c = \frac{a^2 + w_0^2}{2w_0}. \tag{11.11}$$

A reference paraboloid can be defined by the same condition, viz., that the plane $z = 0$ cut its surface in a circle of radius $r = a$. For this to occur, we must have from (11.9):

$$w_0 = \frac{a^2}{4f_P} \quad \Rightarrow \quad f_P = \frac{a^2}{4w_0}. \tag{11.12}$$

From (11.11) and (11.12), it follows that for reference surfaces satisfying these criteria, the radius of curvature of the sphere and the focal length of the paraboloid must be related by the expression

$$R_c = 2f_P + \frac{w_0}{2} = 2\left(f_P + \frac{w_0}{4}\right) \equiv 2f_S, \quad \text{where} \quad f_S \equiv f_P + \frac{w_0}{4}. \tag{11.13}$$

Thus, in the approximation $r \ll R_c$, this reference sphere is approximated not by a paraboloid of focal length f_P, but rather by one of longer focal length f_S. Both focal lengths are determined by the maximum displacement w_0 which, for a given membrane f-number, is obtained from the algorithm leading to equation (8.10). It should be noted that in general *neither* of these focal lengths is the same as the membrane focal length f defined by (8.2).

The last observation suggests a different set of reference surfaces, i.e., we can choose a reference paraboloid having focal length $f_P = f$, and a reference sphere having a radius of curvature that is twice this focal length, i.e., $R_c = 2f$. With these choices, regions near the vertex of any one of the three surfaces will have the *same* focal length.

For either set of reference surfaces, we can compute the deviation $\Delta w(r)$ of the membrane surface from the spherical and paraboloidal reference surfaces, i.e.,

$$\Delta w_S(r) = w(r) - w_S(r) = w(r) - w_0 + R_c - \sqrt{R_c^2 - r^2}, \tag{11.14}$$

and

$$\Delta w_P(r) = w(r) - w_P(r) = w(r) - w_0 + \frac{1}{4f_P}r^2, \tag{11.15}$$

respectively. Since these differences are typically on the order of microns, it is convenient to graph them in units of the wavelength λ of light used to probe the membrane mirror, i.e., we plot

19

$$\Delta w_S(r,\lambda) \;=\; \frac{\Delta w_S(r)}{\lambda} \quad \text{and} \quad \Delta w_P(r,\lambda) \;=\; \frac{\Delta w_P(r)}{\lambda}. \tag{11.16}$$

As an example, Figure 6 is a graph of $-\Delta\widehat{w}_S(\xi,\lambda)$ as a function of ξ for an $f/8$ membrane with three different levels of pre-strain, where we have used the reference sphere that contacts the membrane at both the vertex and the membrane edge. For 0.25% pre-strain, the graph indicates a nearly 95% reduction in the *maximum* deviation from a sphere, which would imply a similar reduction in the spherical aberration of the wavefront reflected from an $f/8$ membrane mirror.
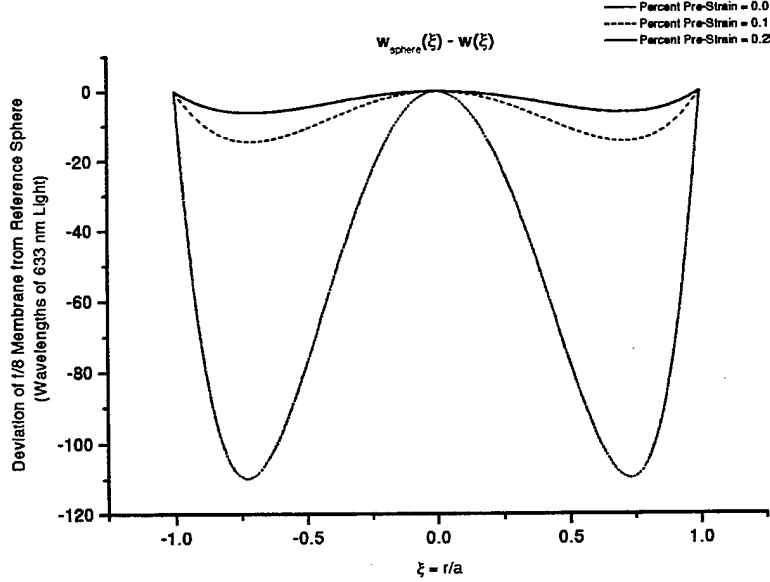

FIG. 6. Deviation of $f/8$ Membrane from Reference Sphere

We are usually interested in this maximum deviation from a reference surface, which occurs at a value of r for which

$$\frac{d}{dr}\big[\Delta w_S(r)\big] = 0 \quad \text{or} \quad \frac{d}{dr}\big[\Delta w_P(r)\big] = 0. \tag{11.17}$$

To determine the left-hand sides of these expressions, we first use the chain rule to compute dw/dr, i.e., we have

$$w(r) \;=\; a\,\widehat{w}(\xi(r)), \quad \text{where} \quad \xi(r) \;=\; \frac{r}{a},$$

hence

$$\frac{dw}{dr} \;=\; a\,\frac{d\widehat{w}}{d\xi}\frac{d\xi}{dr} \;=\; \frac{d\widehat{w}}{d\xi}.$$

However,

$$\widehat{w}(\xi) \;=\; \widehat{W}(\rho(\xi)),$$

so the chain rule can be applied again to obtain

$$\frac{dw}{dr} \;=\; \frac{d\widehat{W}}{d\rho}\frac{d\rho}{d\xi}. \tag{11.18}$$

Recalling from (7.7) that

$$\rho \;=\; f_1\,\xi + f_3\,\xi^3 + f_5\,\xi^5 + \cdots, \tag{11.19}$$

20

we substitute this result together with (6.22) into (11.18), yielding

$$\frac{dw}{dr} = 2\left(f_1 + 3f_3\xi^2 + 5f_5\xi^4 + \dots\right)\frac{\mathcal{C}}{\rho}\sum_{n=1} n\,c_{2n}\,\rho^{2n}, \tag{11.20}$$

where we made the replacement $w_{2n} = \mathcal{C}\,c_{2n}$. It is easy to show that

$$\frac{dw_S}{dr} = -\frac{\xi}{\sqrt{\widehat{R}_c^2 - \xi^2}}, \quad \text{where} \quad \widehat{R}_c \equiv \frac{R_c}{a}, \tag{11.21}$$

and

$$\frac{dw_P}{dr} = -\frac{\xi}{2\widehat{f}_P}, \quad \text{where} \quad \widehat{f}_P \equiv \frac{f_P}{a}, \tag{11.22}$$

hence the value of r or $\xi = r/a$ that will give the maximum deviations must be a solution of either

$$2\sqrt{\widehat{R}_c^2 - \xi^2}\left(f_1 + 3f_3\xi^2 + 5f_5\xi^4 + \dots\right)\mathcal{C}\sum_{n=1} n\,c_{2n}\,\rho^{2n} + \rho\xi = 0, \tag{11.23}$$

or

$$4\widehat{f}_P\left(f_1 + 3f_3\xi^2 + 5f_5\xi^4 + \dots\right)\mathcal{C}\sum_{n=1} n\,c_{2n}\,\rho^{2n} + \rho\xi = 0. \tag{11.24}$$

A graph of the maximum deviation of $f/4$, $f/6$, and $f/8$ membranes from a reference sphere as a function of percent pre-strain is shown in Figure 7, below. The marked improvement (over the zero pre-strain case) to approximately six waves of deviation requires only 0.25% pre-strain for an $f/8$ membrane, but more than 2.0% pre-strain for an $f/4$ membrane.
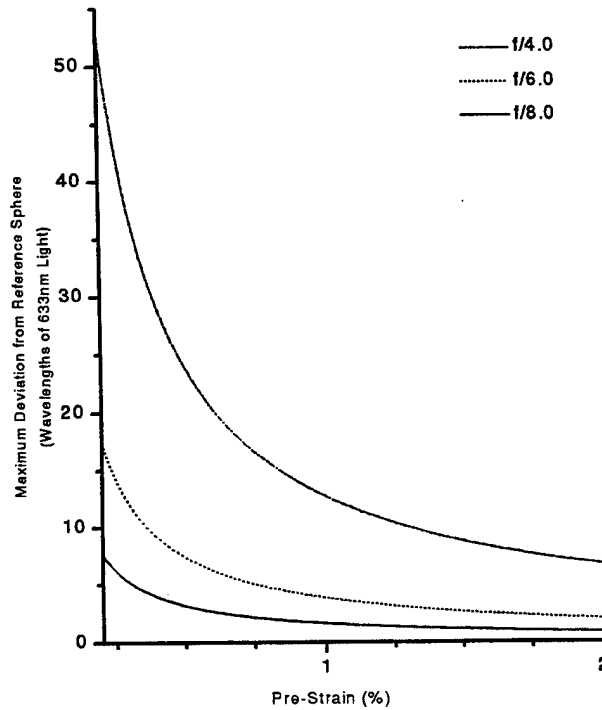

FIG. 7. Maximum Deviation from Reference Sphere-versus-Pre-Strain ($f/4$, $f/6$, and $f/8$ Membranes)

21

XII. RAY DEVIATIONS FROM A MEMBRANE MIRROR ILLUMINATED BY AN ON-AXIS POINT SOURCE

The solution (11.1) for the deformed membrane surface defines a surface of revolution. The equation of such a surface can also be written as

$$\phi(r, z) = 0. \tag{12.1}$$

where the function ϕ is defined by

$$\phi(r, z) \equiv w(r) - z. \tag{12.2}$$

The value of the gradient of this function at a point of the membrane with coordinates (r, z), i.e., $\nabla\phi(r, z)$, is a vector normal to the membrane surface at that point, hence the *unit normal vector* at any such point is given by

$$n = \frac{\nabla\phi}{|\nabla\phi|}. \tag{12.3}$$

Thus, from (12.3) and (12.2), we have for the unit normal to a surface of revolution, expressed in terms of the orthonormal basis $\{e_r, e_\theta, e_z\}$:

$$n(r) = \frac{w'(r)\,e_r - e_z}{\mathcal{D}(r)}, \quad \text{where} \quad \mathcal{D}(r) \equiv \sqrt{[w'(r)]^2 + 1}, \tag{12.4}$$

and the *prime* denotes a derivative with respect to r.

Suppose, now, that an *incident* ray propagating in a direction specified by unit vector k_i strikes a point P of the surface as illustrated in Figure 8. At this point of incidence there will originate, in general, both a *reflected* and a *transmitted* (or *refracted*) ray. The transmitted ray is of no interest here (for a high reflectance surface, the transmitted ray is essentially nonexistent). From Figure 3 and the (geometrical) definitions of the dot and cross products of two vectors, we have

$$n \cdot k_i = \cos(\pi - \theta_i) = -\cos\theta_i, \tag{12.5}$$

$$n \times k_i = \sin(\pi - \theta_i)\,e_\theta = \sin\theta_i\,e_\theta, \tag{12.6}$$

where θ_i is the angle of incidence.

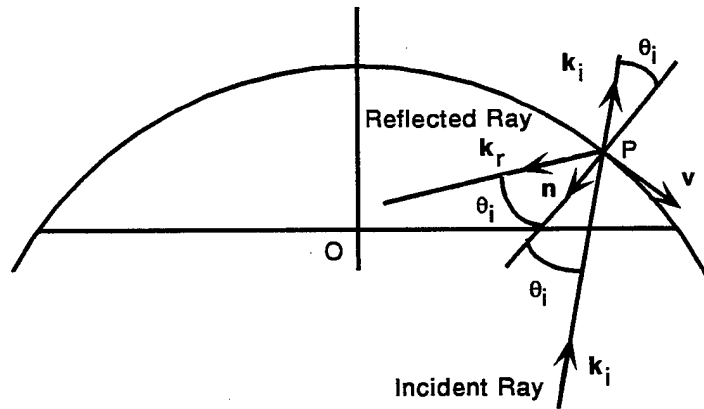FIG. 8. Geometry of Incident and Reflected Rays

22

The direction of the reflected ray is specified by a unit vector k_r. To facilitate the computation of this vector we introduce at P a unit vector v tangent to the meridional curves on the surface, defined by

$$v = n \times e_\theta. \tag{12.7}$$

The unit ray vectors k_i and k_r lie in a plane called the plane of incidence, spanned by the orthonormal pair $\{n, v\}$. Thus, the unit ray vectors can be written in terms of components along n and v as

$$k_i = -\cos\theta_i\, n - \sin\theta_i\, v, \tag{12.8}$$

$$k_r = \cos\theta_i\, n - \sin\theta_i\, v, \tag{12.9}$$

where we used the law of reflection, which states that the angle of reflection equals the angle of incidence θ_i. By subtracting (12.8) from (12.9) and using (12.5) in the result, we obtain $k_r - k_i = 2\cos\theta_i\, n = -2(n\cdot k_i)\, n$, from which

$$k_r = k_i - 2(n\cdot k_i)\, n. \tag{12.10}$$

Equation (12.10) is a coordinate-free expression for the direction of the reflected ray in terms of the given incident direction and the calculated surface unit normal vector.

Referring now to Figure 9, we consider rays emanating from a point source located at C, the center of curvature of *the membrane* (not the reference sphere, as was the case in the previous Section), which has position vector

$$L = -L\, e_z, \qquad L \equiv 2f - w_0, \tag{12.11}$$

with respect to O, as can be easily deduced from the Figure. Any such ray propagates radially outward from C, and we show a particular ray striking the surface at an arbitrary point P, which is then reflected to some point Q.
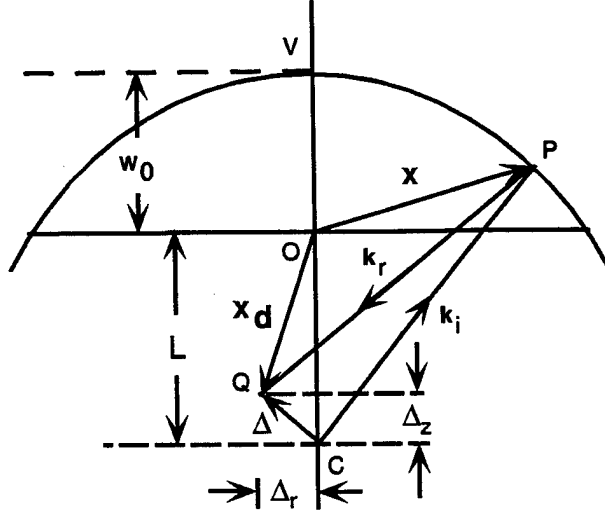

FIG. 9. Ray Deviation Geometry

We denote by

$$x = r\, e_r + z\, e_z = r\, e_r + w(r)\, e_z, \quad \text{where} \quad z = w(r), \tag{12.12}$$

the position vector of P with respect to O, and by x_d the position vector of Q with respect to O, so that

$$x_d = x + d\, k_r = x + d[k_i - 2(n\cdot k_i)\, n], \tag{12.13}$$

where $d = |x_d - x|$ is the *distance* between P and Q along the line parallel to k_r, and (12.10) was used to replace k_r in the final equality.

23

The position vector of Q with respect to C is called the *ray deviation vector*, which we denote by $\boldsymbol{\Delta}$. From Figure 9 we have

$$\boldsymbol{\Delta} = \boldsymbol{x}_d - \boldsymbol{L}, \tag{12.14}$$

hence from (12.13) and (12.14) it follows that

$$\boldsymbol{\Delta} = \boldsymbol{x} - \boldsymbol{L} + d\,[\,\boldsymbol{k}_i - 2\,(\,\boldsymbol{n}{\cdot}\boldsymbol{k}_i\,)\,\boldsymbol{n}\,]. \tag{12.15}$$

For convenience, we introduce a new variable ζ defined by

$$\zeta \equiv z + L = w(r) + L, \tag{12.16}$$

so that

$$\boldsymbol{x} - \boldsymbol{L} = r\,\boldsymbol{e}_r + z\,\boldsymbol{e}_z + L\,\boldsymbol{e}_z = r\,\boldsymbol{e}_r + \zeta\,\boldsymbol{e}_z. \tag{12.17}$$

Now, the incident ray unit vector $\boldsymbol{k}_i$ in this case is just a unit vector along the position vector of P with respect to C, i.e.,

$$\boldsymbol{k}_i = \frac{\boldsymbol{x} - \boldsymbol{L}}{|\boldsymbol{x} - \boldsymbol{L}|} = \frac{\boldsymbol{x} - \boldsymbol{L}}{\mathcal{D}_C}, \quad \text{where} \quad \mathcal{D}_C(r,\zeta) \equiv \sqrt{r^2 + \zeta^2}\,. \tag{12.18}$$

Substituting (12.18) in (12.15) yields

$$\boldsymbol{\Delta} = \boldsymbol{x} - \boldsymbol{L} + \frac{d}{\mathcal{D}_C}\{\,(\,\boldsymbol{x} - \boldsymbol{L}\,) - 2\,[\,\boldsymbol{n}{\cdot}(\,\boldsymbol{x} - \boldsymbol{L}\,)\,]\,\boldsymbol{n}\,\}. \tag{12.19}$$

The radial and lateral components of the ray deviation vector are thus

$$\Delta_r = \boldsymbol{e}_r{\cdot}\boldsymbol{\Delta} = r + \frac{d}{\mathcal{D}_C}\{\,r - \frac{2\,w'}{\mathcal{D}}\,[\,\boldsymbol{n}{\cdot}(\,\boldsymbol{x} - \boldsymbol{L}\,)\,],$$

$$\Delta_z = \boldsymbol{e}_z{\cdot}\boldsymbol{\Delta} = \zeta + \frac{d}{\mathcal{D}_C}\{\,\zeta + \frac{2}{\mathcal{D}}\,[\,\boldsymbol{n}{\cdot}(\,\boldsymbol{x} - \boldsymbol{L}\,)\,],$$

or, since $\boldsymbol{n}{\cdot}(\,\boldsymbol{x} - \boldsymbol{L}\,) = (\,r\,w' - \zeta\,)/\mathcal{D}$, we have

$$\Delta_r = r + \frac{d}{\mathcal{D}_C}\,[\,r - \frac{2\,w'}{\mathcal{D}^2}\,(\,r\,w' - \zeta\,)\,], \qquad \Delta_z = \zeta + \frac{d}{\mathcal{D}_C}\,[\,\zeta + \frac{2}{\mathcal{D}^2}\,(\,r\,w' - \zeta\,)\,].$$

Factoring $1/\mathcal{D}^2$ from the square-bracketed terms, recalling that $\mathcal{D}^2 = (w')^2 + 1$, these can also be written as

$$\Delta_r = r + 2\,\frac{d}{\mathcal{D}^2\mathcal{D}_C}\,(\,\zeta\,w' + r\alpha\,), \qquad \Delta_z = \zeta + 2\,\frac{d}{\mathcal{D}^2\mathcal{D}_C}\,(\,r\,w' - \zeta\,\alpha\,), \tag{12.20}$$

where we have introduced for convenience:

$$\alpha \equiv \frac{1}{2}\,[\,1 - (w')^2\,]. \tag{12.21}$$

The factor $d/\mathcal{D}^2\mathcal{D}_C$ can be eliminated between the two equations of (12.20), yielding the following relation between the ray deviation components:

$$\Delta_r = \frac{\zeta\,w' + r\alpha}{r\,w' - \zeta\,\alpha}\,\Delta_z + \frac{(\,r^2 - \zeta^2\,)\,w' - 2\,r\,\zeta\,\alpha}{r\,w' - \zeta\,\alpha}. \tag{12.22}$$

For a given value of the longitudinal deviation Δ_z, we can use (12.22) to graph the transverse deviation Δ_r as a function of the coordinate r of the point P on the membrane from which the ray was reflected.

It is also useful to compute the *angular deviation* δ of a reflected ray from the incident ray. This deviation is just twice the angle of incidence, i.e., $\delta \equiv 2\,\theta_i$. From (12.5), (12.6), (12.4), and (12.18), we have

$$\boldsymbol{n}{\cdot}\boldsymbol{k}_i = -\cos\theta_i = \frac{1}{\mathcal{D}\mathcal{D}_C}\,(\,r\,w' - \zeta\,), \tag{12.23}$$

$$\boldsymbol{n}{\times}\boldsymbol{k}_i = \sin\theta_i\,\boldsymbol{e}_\theta = -\frac{1}{\mathcal{D}\mathcal{D}_C}\,(\,\zeta\,w' + r\,)\,\boldsymbol{e}_\theta, \tag{12.24}$$

hence the ray deviation angle is given by

$$\delta = 2\,\theta_i = 2\,\tan^{-1}\!\left(\frac{\zeta\,w' + r}{r\,w' - \zeta}\right). \tag{12.25}$$
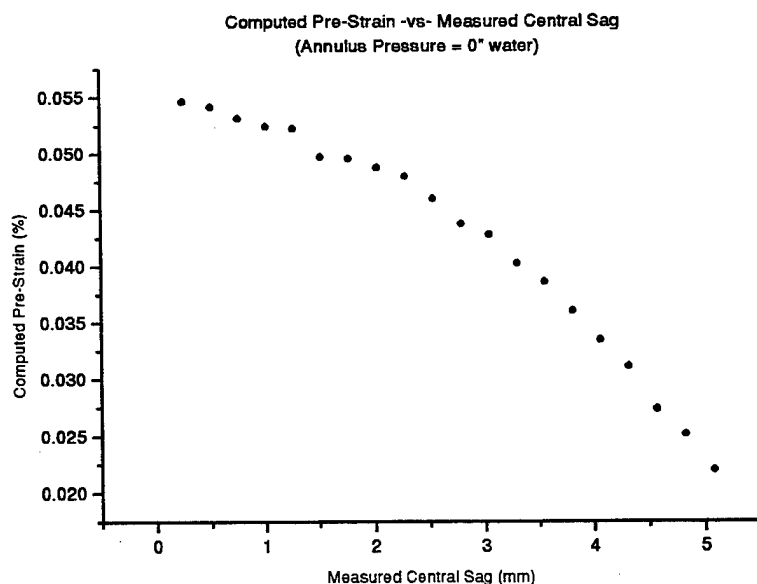
24

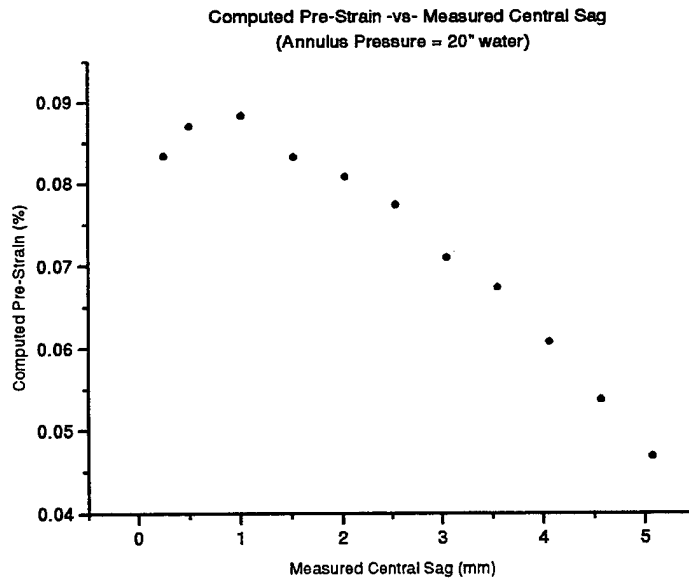# XIII. COMPARISONS WITH LABORATORY MEASUREMENTS

Two types of measurements were made [10] on an 11-inch ($\sim$ 28-cm) diameter laboratory membrane of 125 μ thick Upilex, having a Young's modulus of $E = 8800\,N/m^2$ and a Poisson's ratio of $\nu = 0.4$. In the first type of measurement, the annulus vacuum pressure was fixed at some value ($p_0 = 0$ inches of water in one case, and $p_0 = 20$ inches of water in the other case), and the central displacement (sag) w_0 was measured as the inner membrane vacuum pressure p was increased. A measurement of inner membrane pressure was recorded at every 0.010-inch (10 mil) increment of the central sag as shown in the following tables:

$p_0 = 0$ inches water

| w_0 (mm)	p (inches water)
0.254	0.21
0.508	0.42
0.762	0.63
1.016	0.85
1.270	1.09
1.524	1.30
1.778	1.58
2.032	1.87
2.286	2.19
2.540	2.50
2.794	2.83
3.048	3.25
3.302	3.64
3.556	4.12
3.810	4.60
4.064	5.13
4.318	5.73
4.572	6.30
4.826	7.03
5.080	7.77

$p_0 = 20$ inches water

| w_0 (mm)	p (inches water)
0.254	0.32
0.508	0.67
1.016	1.40
1.524	2.07
2.032	2.85
2.54	3.70
3.048	4.54
3.556	5.65
4.064	6.78
4.572	8.08
5.08	9.62

For each data point (w_0, p), the Hencky-Campbell theory was used to compute the predicted pre-strain ϵ existing in the inner membrane. These computed values are plotted versus the measured central sag in the following two graphs.

Computed Pre-Strain -vs- Measured Central Sag
(Annulus Pressure = 0" water)

Computed Pre-Strain -vs- Measured Central Sag
**(Annulus Pressure = 20" water)**

These graphs show that although the annulus pressure was maintained at a nearly constant value, the amount of strain in the inner membrane attributable to the "pre-strain" occurring in the Hencky-Campbell theory decreases as the inner membrane vacuum pressure is increased. This is not surprising since the laboratory membrane is not clamped on the inner ring, hence an increase in inner membrane pressure can cause some of the membrane material over the annulus chamber to slip across the inner ring to become part of the inner membrane. The effect of this membrane migration is a reduction of the total strain in the inner membrane (compared to the strain that would exist if the membrane had been clamped on the inner ring), which manifests in the model as a reduction of the effective pre-strain. The next two graphs are plots of the inner membrane pressure against central sag, where the points are the data points from the tables on the last page, and the curves reflect model predictions using the *mean value* (not a particularly good estimator) of the computed pre-strains shown in the previous two graphs.

Pressure -vs- Central Sag
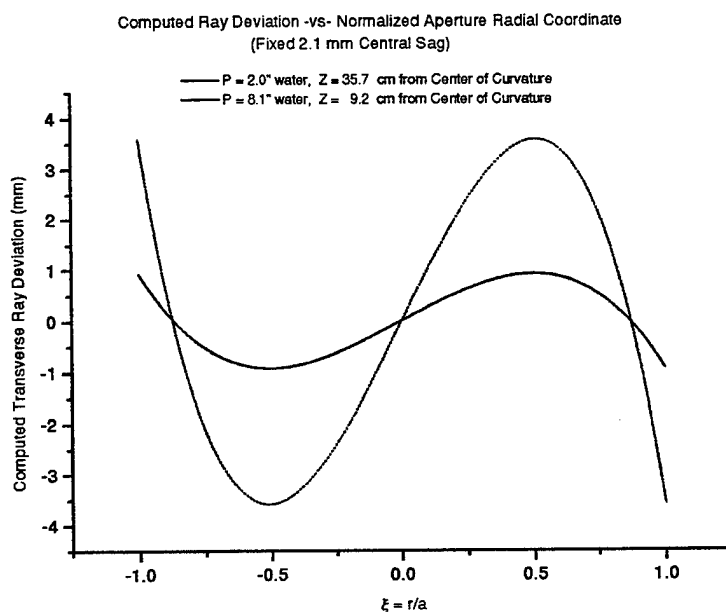(Annulus Pressure = 20" water)
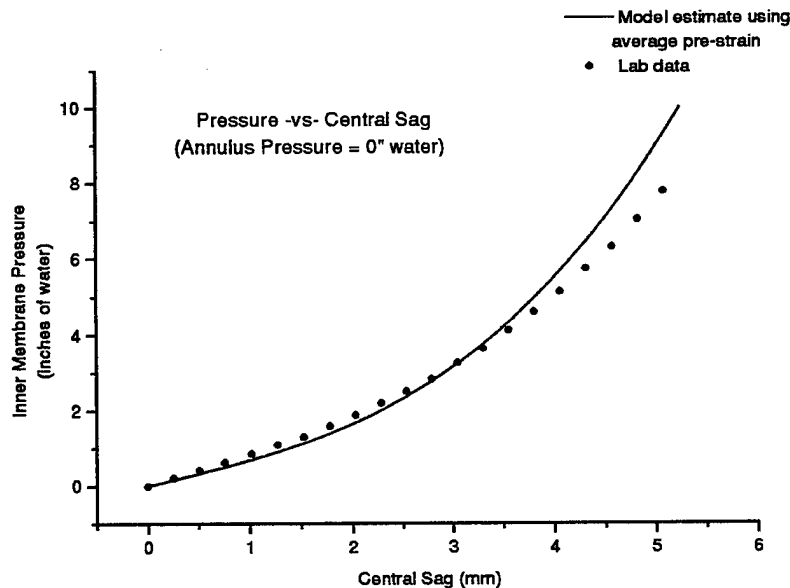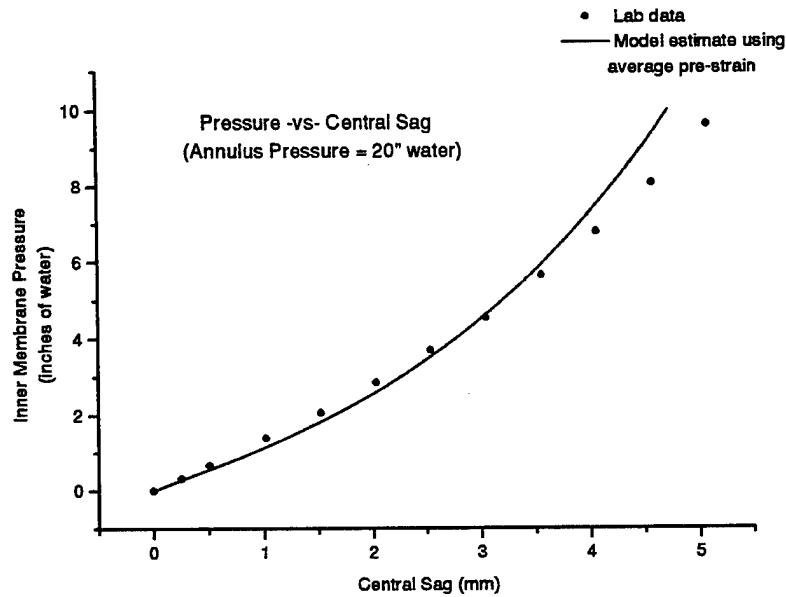
In the second type of measurement the inner membrane vacuum pressure was adjusted until the central deflection was $w_0 = 2.1$ mm. This was done for two different annulus vacuum pressures. The inner membrane vacuum pressure required for the low annulus pressure case was $p = 2.0$ inches of water, while the high annulus pressure case required a pressure of $p = 8.1$ inches of water. These data were used to calculate pre-strains of 0.05% and 0.24%, respectively. The predicted deviations of the membrane surfaces from a reference sphere (contacting the membrane at its vertex and along the inner ring) in the two examples is shown in the next graph. The effect of a higher pre-strain on the shape is rather dramatic, causing the maximum deviation to be reduced from over 22 waves to about 6 waves.
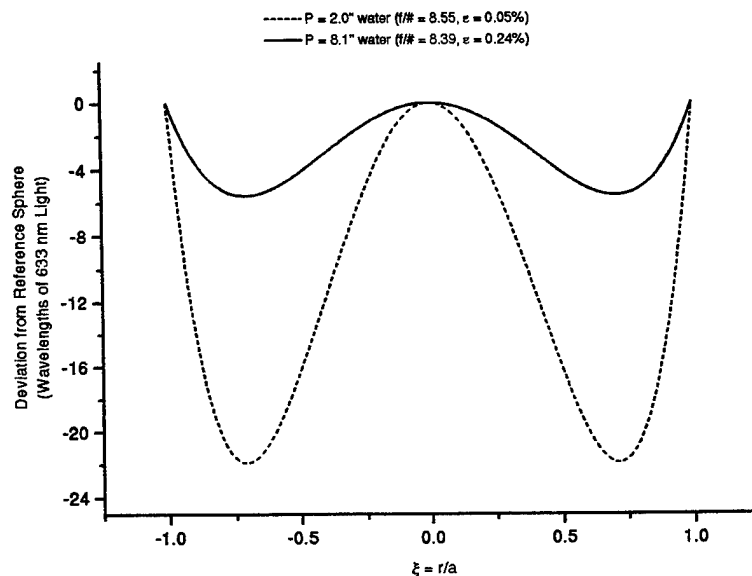
In each case the membrane mirror was being illuminated by laser light from a pinhole (simulated point source) located at the center of curvature of the membrane. Measurements were made of the minimum geometric spot size of the

light reflected from the mirror. The measured minimum spot size was roughly 7-8 mm for the low pre-strain case, and 3-4 mm for the higher pre-strain. In the next graph we show plots of the computed transverse ray deviations in the z-planes where the maximum transverse ray deviations were minimized ($z = 35.7$ cm and $z = 9.2$ cm from the membrane center of curvature for the low and high pre-strain, respectively).

Computed Ray Deviation -vs- Normalized Aperture Radial Coordinate
(Fixed 2.1 mm Central Sag)

——— P = 2.0" water, Z = 35.7 cm from Center of Curvature
——— P = 8.1" water, Z = 9.2 cm from Center of Curvature

The predicted peak-to-valley ray deviations, which correspond directly to the spot diameters, are seen to be on the order of 7 mm and 2 mm, respectively, somewhat smaller than the measured spot diameters. This is to be expected, since our axially symmetric model does not account for asymmetric aberrations observed in the laboratory membrane (especially astigmatism), which contribute to the larger measured spot sizes.

[1] Campbell, J. D., *Quart. J. Mech. and Appl. Math.* IX, 84-93, 1956.

[2] Fichter, W. B., NASA Technical Paper 3658, July 1997.

[3] Fung, Y. C., *Foundations of Solid Mechanics*, Prentice-Hall, Englewood Cliffs, 1965.

[4] Greschik, G., Mikulas, M. M., and Palisoc, A., Proceedings of the 39th Structures, Structural Dynamics, and Materials Conference and Adaptive Structures Forum, Long Beach, CA, April 20-23, 1998. Volume 4, 2772-2782, AIAA. AIAA-98-2101-CP.

[5] Hencky, H., *Zeitschrift für Mathematik und Physik* 63, 311-317, 1915.

[6] Marker, D. K., Carreras, R. A., and Jenkins, C. H., Second International Symposium on Intelligent Automation and Control, World Automation Congress (WAC), 9-14 May 1998, Anchorage, Alaska.

[7] Marker, D. K., Carreras, R. A., Wilkes, J. M., and Jenkins, C. H., Ninth Annual Conference Laser Optics 98, Vavilov State Optical Institute, 22-26 June 1998, St. Petersburgh, Russia.

[8] Press, W. H., Flannery, B. P., Teukolsky, S. A., and Vetterling, W. T., *Numerical Recipes: The Art of Scientific Computing*, Cambridge University Press, New York, 1986.

[9] Rotge, J. R., Marker, D. K., Carreras, R. A., Jenkins, C. H., Wilkes, J. M., Duneman, D., SPIE, 20-27 July 1998, San Diego, California.

[10] Rotge, J. R., private communication.

[11] von Kármán, T., *Encyklopädie der Mathematischen Wissenschaften* IV, 349, 1910.

DISTRIBUTION LIST

AUL/LSE
Bldg 1405 - 600 Chennault Circle
Maxwell AFB, AL 36112-6424   1 cy

DTIC/OCP
8725 John J. Kingman Rd, Suite 0944
Ft Belvoir, VA 22060-6218   2 cys

AFSAA/SAI
1580 Air Force Pentagon
Washington, DC 20330-1580   1 cy

AFRL/PSTL
Kirtland AFB, NM 87117-5776   2 cys

AFRL/PSTP
Kirtland AFB, NM 87117-5776   1 cy

AFRL/DE/Dr. Good
Kirtland AFB, NM 87117-5776   1 cy

Official Record Copy
 AFRL/DEBS/James M. Wilkes   10 cys